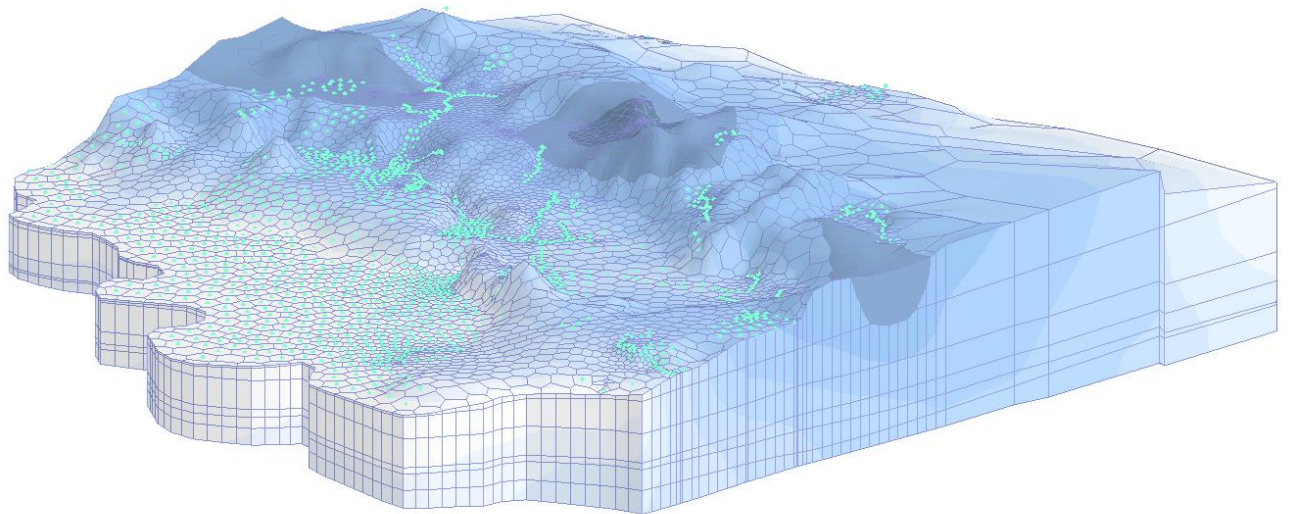


Waiharara-Paparore Groundwater Model

Factual Technical Report - Modelling

TIRI AVOCADOS LTD; VALIC NZ LTD; WATAVIEW ORCHARD
WWA0045 | Rev 2_Final

3 August 2018





Motutangi-Waiharara Groundwater Model

Project no: WWA0045
 Document title: Groundwater Modelling Analysis
 Revision: Rev 2_Final
 Date: 3 August 2018
 Client name: Tiri Avocados Ltd.; Valic NZ Ltd.; Wataview Orchard
 Project manager: Jon Williamson
 Author(s): Jacob Scherberg, Hangjian Zhao and Jon Williamson
 File name: G:\Team Drives\Projects\Murray Forlong\WWA0045_Waiharara-Paparore Model\Deliverables\Waiharara-Paparore Groundwater Model_v2 Final.docx

Williamson Water Advisory

PO Box 314,
 Kumeu 0841,
 Auckland
 T +64 21 654422

Document history and status

Rev	Date	Description	By	Review	Approved
1	30 July 2018	Internal review		Jon Williamson	
2	3 August 2018	Final review	Jake Scherberg		Jon Williamson

Distribution of copies

Rev	Date issued	Issued to	Comments
2	3 August 2018	Clients and Northland Regional Council	

Contents

Executive Summary	6
1. Introduction	1
1.1 Report Structure	1
2. Model Conceptualisation	3
2.1 Soils	3
2.2 Geology	3
2.3 Aquifer Hydraulic Parameters	6
2.3.1 Perched Aquifers and Aquifer Confinement	6
2.4 Recharge	7
2.4.1 Background Data	7
2.5 Drainage	7
2.6 Groundwater Level Data	7
2.7 Groundwater Abstraction	8
2.7.1 Actual Use Dataset	8
3. Model Configuration	10
3.1 Model Domain	10
3.1.1 Constant Head Boundaries	10
3.1.2 General Head Boundaries	10
3.1.3 No-Flow Boundaries	10
3.1.4 Drain Boundaries	11
3.1.5 Well Boundaries	11
3.2 Simulation Package	11
3.2.1 Sparse Matrix Solver	11
3.2.2 Ghost Node Correction Package	11
3.3 Model Layer Configuration	11
3.3.1 Layer Geology	11
3.3.2 Layer Elevations	12
4. Model Calibration	15
4.1 Observation Points	15
4.2 Steady-State Calibration	16
4.3 Transient Calibration	17
4.3.1 Stress Periods and Time Steps	17
4.3.2 Groundwater Pumping	17
4.3.3 Initial Conditions	17
4.3.4 Model Parameters	17
4.4 Calibrated Model Output	18
4.4.1 Groundwater Levels	18
4.4.2 Model Flow Budget	19

5.	Predictive Simulations	21
5.1	Scenario Setup.....	21
5.2	Model Results	21
5.2.1	Mass Balance.....	21
5.2.2	Drain Flows	23
5.2.3	Water Level Impacts	24
5.2.4	Drawdown Effects	27
5.2.5	Saltwater Intrusion	29
5.2.5.1	Lateral Migration Analysis	29
6.	Conclusions	33
7.	References.....	35

Figures

Figure 1. Project locality map. (See A3 attachment at rear).	1
Figure 2. Lithological unit classification from example borelogs.	Error! Bookmark not defined.
Figure 3. Drainage map. (See A3 attachment at rear).	7
Figure 4. Location of monitoring piezometers. (See A3 attachment at rear).	8
Figure 5. Mean groundwater levels of monitoring piezometers nests in the model area.	8
Figure 6. Location of existing and proposed groundwater take bores. (See A3 attachment at rear).	8
Figure 7. Simulated groundwater extraction (m ³ /annum partial groundwater use in 2016 due to the end of the model simulation).	9
Figure 8. Plan view of unstructured model grid discretisation (See A3 attachment at rear).	10
Figure 9. Basement rock elevation contours (model Layer 6 base). (See A3 attachment at rear).	12
Figure 10. Hydrogeological cross section locations. (See A3 attachment at rear).	12
Figure 11. Interpolated cross-section at N-S (1).	13
Figure 12. Interpolated cross-section at N-S (2).	13
Figure 13. Interpolated cross-section at E-W (1).	14
Figure 14. MODFLOW grid with vertical magnification of 10.	14
Figure 15. Simulated head versus observed head.	16
Figure 16. Surface drainage low flow analysis for model predictive scenarios.	24
Figure 17. Locations for scenario groundwater level analysis (See A3 attachment at rear).	24
Figure 18. Groundwater level hydrographs for North reference location	25
Figure 19. Groundwater level hydrographs for Centre reference location.	26
Figure 20. Groundwater level hydrographs for South reference location.	27
Figure 21. Simulated drawdown of deep aquifer (Scenario 2). (See A3 attachment at rear).	28
Figure 22. Simulated drawdown of deep aquifer (Scenario 3). (See A3 attachment at rear).	28
Figure 23. Simulated drawdown of shallow aquifer (Scenario 2). (See A3 attachment at rear).	28
Figure 24. Drawdown observed at existing bores at the observation time step for each scenario.	29
Figure 25. Location of the selected points for lateral migration analysis (see A3 attachment at rear).	29
Figure 26. Simulated minimum groundwater level between 1956 and 2016 in Layer 6 (East Coast, NE to SE).	31
Figure 27. Simulated minimum groundwater level between 1956 and 2016 in Layer 6 (West Coast, SW to NW).	31
Figure 28. Simulated groundwater level in Layer 6 at coastal point 11.	32

Executive Summary

Williamson Water Advisory (WWA) were commissioned by the Tiri Avocados Ltd., Valic NZ Ltd., and Wataview Orchard to develop a numerical model and prepare an assessment of effects report for three proposed groundwater take resource consent applications. The participants are seeking both increases and new groundwater takes for avocado orchard irrigation that total 5,259 m³/day.

A numerical groundwater flow model was developed to determine the potential impact from the proposed groundwater abstraction on the regional aquifer system and the hydrological condition of relevant surface water. In particular, the model was used to define the potential impact from seasonal pumping on the aquifer system water budget, aquifer groundwater levels, surface water drain flows, and the position of the saltwater/fresh water interface.

Three scenarios were developed and simulated with the model representing a) the current base case; b) the future given the proposed takes assuming a leaky aquifer model, and c) the future given the proposed takes assuming a relatively non-leaky aquifer model.

This report presents the factual results of the modelling study, while an accompanying Assessment of Environmental Effects report analyses and interprets the results from a Resource Management Act perspective.

1. Introduction

Williamson Water Advisory (WWA) has been commissioned by the three individual property owners (Tiri Avocados Ltd; Valic NZ Ltd; Wataview Orchard) to develop a numerical model and prepare an assessment of environmental effects (AEE) report addressing the environmental effects from proposed groundwater abstractions for avocado irrigation. This assessment includes effects on:

1. Groundwater level
2. Neighbouring bores
3. Groundwater availability
4. Saline intrusion
5. Surface waterways
6. Land subsidence (addressed separately in an AEE report).

WWA's scope of work included:

Data Review - Review and update of the lithological characteristics of the subsurface profile from bore logs and aquifer hydraulic parameters as determined from recent test pumping where available.

Groundwater modelling - Development of a calibrated three-dimensional groundwater model using MODFLOW, to enable assessment of:

- Groundwater level and availability;
- Interference effects on individual bores;
- Cumulative effects on surface water features (streams, lakes and swamps); and
- Saline intrusion.

Reporting - Preparation of a comprehensive report and associated maps.

The extent of the model domain and location of the current and proposed groundwater takes within the model boundary along with other key features of the area are shown in **Figure 1**.

Figure 1. Project locality map. (See A3 attachment at rear).

This report presents the factual results of the modelling study, while an accompanying Assessment of Environmental Effects report analyses and interprets the results from a Resource Management Act perspective.

1.1 Report Structure

The structure of this technical report is as follows:

- **Section 2** provides an overview of the conceptualisation of the groundwater flow model, including a discussion of the results from field survey of bore levels.
- **Section 3** details the model construction and configuration.

- **Section 4** details the calibration of the steady-state and transient models.
- **Section 5** details the setup and results from predictive simulations.
- **Section 6.** provides a summary of the key findings and conclusions of this project.

2. Model Conceptualisation

This section describes the conceptualisation of regional hydrogeological conditions and the methods applied in representing these conditions in the numerical groundwater flow model.

2.1 Soils

The western to central part of the project area is predominately comprised of sandy brown soils. Along both coastal strips there are coastal dunes, which are unconsolidated and windblown with little to no soil development, and excessively drained.

The eastern area is mixed with a variety of peat, sand and pockets of clay soils. The prevalent soils in the eastern areas are loamy peat and peaty sand. The loamy peat soils are organic, characterised by high water available capacity and low bulk density. The peat in these soils is moderately decomposed.

The peaty sand soils are pan podzols, which have cemented pans within the B horizon and have naturally low fertility and low permeability, limiting root depth.

It is interesting to note that most boreholes display units of peat and iron pan at multiple depths, suggesting the sand dune sequences have shifted in location and hence are highly dynamic through geological time.

Long-time local farmers and orchard developers provided the following anecdotal information on iron pans:

- “The iron pans vary in both thickness and number of layers” (pers. com. Stanisich, Broadhurst, Hayward).
- “There are multiple layers of pan at varying depths and our pan breaking for planting rows only seems to create vertical drainage at the top” (pers. com. McClarnon).
- “Monitoring of bores screened in different zones during test pumping often show no effect at shallower levels to the pumping bore, indicating some separation of zones” (pers. com. Stanisich, Hayward).
- “From bore logs, iron pans are often recorded as consolidated brown sands. However, these may not be the only confining layers. Consolidated mica sands and silts are also good barriers” (pers. com. Stanisich).

2.2 Geology

The geology of the Waiharara-Paparore area consists of Pleistocene and Holocene unconsolidated sedimentary materials deposited in beach and dune (abandoned shorelines and marine terraces) and associated alluvial, intertidal estuarine, shallow marine, lakebed and wetland environments.

The geologic units in the model domain were identified through the available bore logs sourced from NRC. The sediments near the surface typically comprise fine-grained sands, interspersed with sporadic iron pan, peat, lignite, silt, gravel and shellbeds.

With distance inland from the coast, the sand deposits become progressively older and have a higher degree of compaction and weathering compared to the younger foredune sands located at the coast.

With increasing depth, the occurrence of shellbed layers increases. The shellbeds comprise layers that typically range in composition from 30-90% medium to coarse shell and 10-70% fine sand. The shellbed aquifer typically resides from approximately 70 to 120 mBGL, and is the most prolific water yielding aquifer in the region and hence the target for irrigation bores.

Underlying the shellbed aquifer are basement rocks of the Mount Camel Terrain, which typically comprise hard grey to dark green / black igneous rocks described in Isaac (1996) as intercalated basalt and basaltic andesite lava, pillow lava, rhyolitic tuff, tuff-breccia, conglomerate, sandstone and mudstone.

Drilling data in the Waiharara-Paparore area indicates that the sedimentary sequence can be broadly classified into two lithological units. The upper bulk layer comprises the fine-grained sands, interspersed with iron pan, peat, lignite, and silt. The lower layer comprises mostly shell beds, although recent drilling has identified the existence of two discrete shell units separated by a thin fine sand or silt layer. The lithological unit classification

developed for this study is exemplified in

TIRI AVOCADOS LTD; VALIC NZ LTD; WATAVIEW ORCHARD
Waiharara-Paparore Groundwater Model



Valic-1
(Drilled on 16 August 2006)

From (mBGL)	To (mBGL)	Lithology	Model layers
0	1	Fine sand-brown	Layer 1 - Sand/Silt
1	2	Fine sand-dark brown	
2	4	Fine sand-light brown/grey	
4	6	Fine sand-light orange/brown	
6	13	Fine sand-light orange/brown. Trace organics	
13	15.5	Fibrous peat with wood/roots. Black	
15.5	18	Fine sand-dark brown/grey. Siliceous. Trace mica	
18	20	As above-becoming greyish brown	
20	26	Fine sand-dark brown/grey. Siliceous. Trace mica	
26	29	Amorphous peat, dark brown/black	
29	33	Fine sand, dark brown/brownish grey	
33	45	Fine sand, dark brown/brownish grey. Minor medium to coarse sand (quartz/silica). Trace mica	
45	52	Fine to medium sand-grey	
52	56	Medium sand, greyish brown. Minor coarse sand quartz/silica and mica	
56	62	Fine sand-orange brown	
62	67	Fine sand as above becoming grey	
67	68	Fine-med brown	
68	75	Fine sand, greenish grey, glauconitic, siliceous, minor mica	
75	83	Fine sand-greenish grey with minor mica; glauconitic, siliceous	
83	85	Fine sand as above. Trace fine shell	
85	86	As above, coarser shell	
86	88	Fine grey sand. Coarse shell up to 40%	
88	90	Fine sand. 10% Coarse shell	
90	93	Silty fine sand with marine mud. Trace fine to coarse shell	
93	98	Silty fine sand with marine mud. Coarse shell 10-40% increasing with depth	
98	100	Coarse granular shell (65%) with fine grey	
100	108	Fine sand, grey, 10% shell	
108	117	Fine sand, grey, trace shell	

George Ujdar Bore
(Drilled on 06 April 2006)

From (mBGL)	To (mBGL)	Lithology	Model layers
0	5	Topsoil/brown-grey sand	Layer 1 - Sand/Silt
5	48	Brown/grey sands	
48	55	Grey sand	
55	74	Brown Sand	
74	87	Compacted grey sand	
87	92	Brown sand with peate and shell	
92	97	Coarse shell	
97	101	Fine shell with fine sand	
101	104	Coarse shell	
104	105	Basement rock	

Largus Orchard Bore
(Drilled on 12 April 2017)

From (mBGL)	To (mBGL)	Lithology	Model layers
0	1	Golden dune sand	Layer 1 - Sand/Silt
1	4.5	Peat and timber	
4.5	18	Brown/green fine sands	
18	42.7	Grey/white sands	
42.87	45.5	Firm grey sandy silts	
45.5	47	Brown peaty silts	
47	53	Brown/grey fine sands	
53	63	Green/grey fine sands, some thin bands fine gravel	
63	67.5	Sandy silt, flecks of shell	
67.5	68.5	Cleaner silt, shell	
68.5	73	Grey silt	
73	74.1	Cleaner sand, shell	
74.1	76	60% Coarse shell	
76	77	20% Coarse shell	
77	78	50% Coarse shell	
78	80	20% Coarse shell	
80	83	70% Coarse shell	
83	84	50% Coarse/med shell	
84	86	50% Medium shell	
86	88	30% Medium shell	
88	89	50% Medium shell	
89	91	30% Medium shell	
91	93.6	50% Coarse/med shell	
93.6	93.8	Light green silt	
93.8	105	Firm, clean, grey/white shell rock	
105	106	Softer mushy shell rock	
106	107	Clean firm shell rock	
107	110.9	Softer mushy shell rock	

using three reliable bore logs, and is described as follows:

- **Layer 1 – Sand / Silt.** A sequence of predominately unconsolidated fine sand intersperses with discontinuous layers of alternating iron pan, silt and peat. The layer varies in thickness from approximately 45 m to 110 m with the thickest regions located around the model area peak elevations.
- **Layer 2 – Upper Shellbed.** A sequence of shellbeds comprising medium to coarse shell with some fine sand in the matrix. The proportion of shell typically varies from 30% to 90%. The layer is typically encountered at a depth of 60 - 110 mBGL and varies in thickness from typically 5 m to 15 m.
- **Layer 3 – Sand.** A thin layer of finer sediment separating the upper and lower shellbed.
- **Layer 4 – Lower Shellbed.** A sequence of shellbeds typically comprising a higher proportion of shell and coarser grain size than the upper shellbed. In some locales, the shell is more consolidated and described by drillers as shellrock. Drillers also report circulation losses when drilling this formation. The layer is typically encountered at depths of 80 - 145 mBGL and varies in thickness from typically 5 m to 30 m.

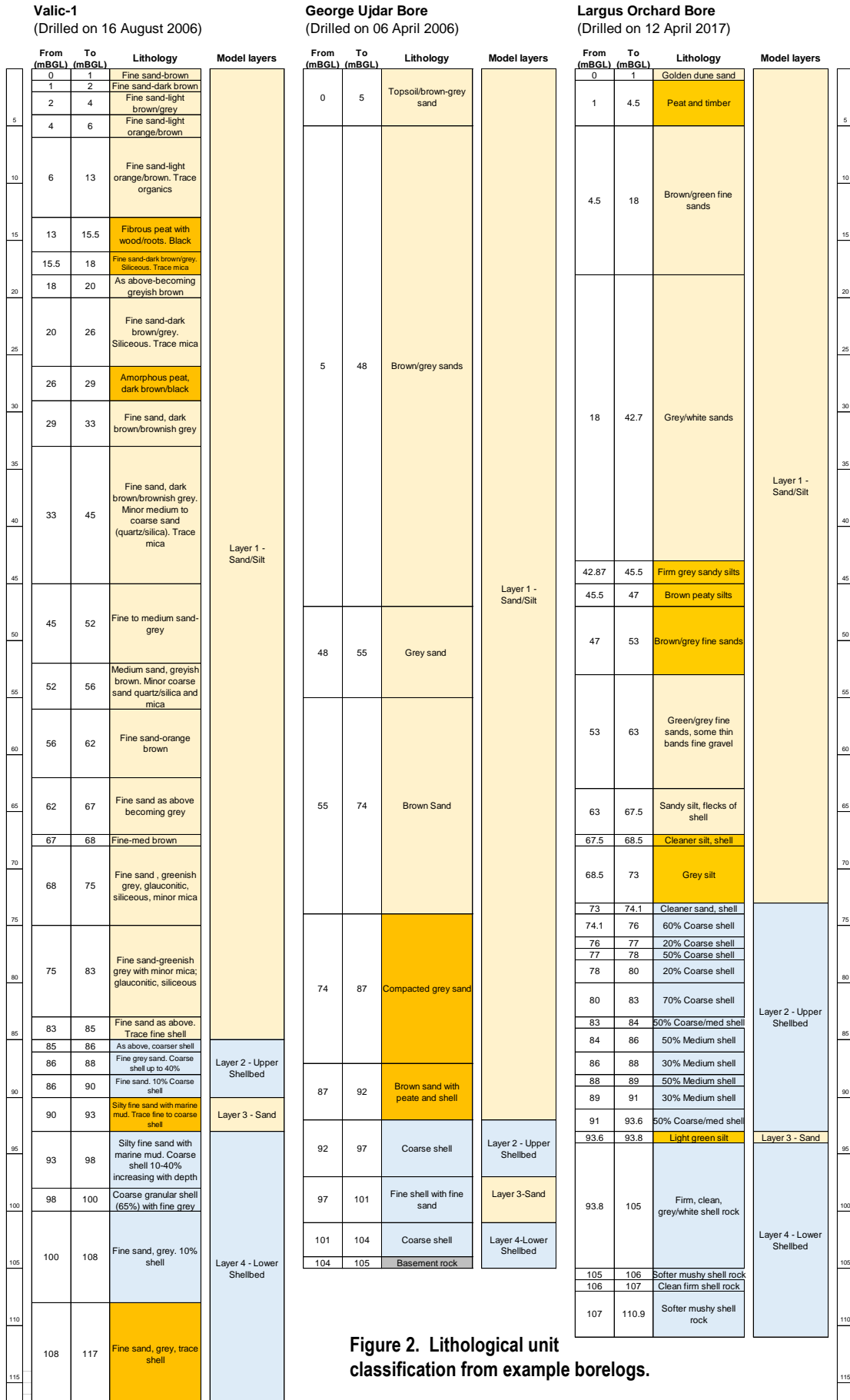


Figure 2. Lithological unit classification from example borelogs.

2.3 Aquifer Hydraulic Parameters

Groundwater is found throughout the unconsolidated sedimentary materials that occur within the model area, although these mater materials vary in their ability to store and transmit water, primarily due to grain size, cementation, weathering and compaction.

Test pumping and numerical modelling exercises for irrigation take resource consent applications have been undertaken over the years and summarised in the reports of HydroGeo Solutions (2000), SKM (2007a), SKM (2010), Lincoln Agritech (2015) and most recently by Williamson Water Advisory in 2017 (WWA, 2017). Data from these reports has been reproduced in tables provided in 7, and is summarised below in **Table 1** where it is presented in the context of our conceptual model as described in the previous section of this report.

Table 1. Summary of previously measured and modelled hydraulic properties for WWA layer conceptualisation.

Unit	K _x (m/s)			S (-)		
	Min	Max	Arithmetic Mean	Min	Max	Arithmetic Mean
Layer 1 - Sand / silt	1.0x10 ⁻⁵	1.1x10 ⁻⁴	8.4x10 ⁻⁴	2x10 ⁻²	1.5x10 ⁻²	9.6x10 ⁻³
Layer 2 – Upper shellbed	2.1x10 ⁻⁴	7.3x10 ⁻⁴	3.65x10 ⁻⁴	2x10 ⁻²	4x10 ⁻⁴	3x10 ⁻⁴
Layer 3 - Sand	Assume same as Layer 1			Assume same as Layer 1		
Layer 4 – Lower shellbed	1.3x10 ⁻⁴	7.3x10 ⁻⁴	4.4x10 ⁻⁴	3x10 ⁻⁴	4.4x10 ⁻³	1.6x10 ⁻³

2.3.1 Perched Aquifers and Aquifer Confinement

There is anecdotal evidence of localised perched water within the wetlands and lakes in the area. For example, Lake Waiparera, located on the north boundary of the study area has an average lake stage of 33.8 mAMSL, yet the groundwater level estimated from an adjacent bore is around 7 mAMSL.

Before the intervention of man, lake and wetland complexes that formed in dune swales were self-accentuating over time. As fine sediment was washed into the swale with stormwater runoff, bed permeability progressively decreased due to clogging, which led to widening and deepening of the wetland or lake. As this progressed, acid conditions in the wetland environment led to dissolution of metals and as the sediment substrate conditions shifted from aerobic to anaerobic (or reducing conditions) and pH became more neutral, subsequent precipitation of the dissolved metals occurred as metal hydroxides, particularly iron hydroxide. Iron hydroxide is the primary constituent of iron humus pan or iron pan, which is the main factor (along with peat and silt deposits) in restricting vertical drainage in the Aupouri aquifer.

The aquifer system is unconfined at the surface but behaves in a manner that suggests a progressive degree of confinement with depth (leaky confinement). There is no well-defined regionally extensive confining layer but there are numerous low-permeability layers (e.g. iron pan, brown (organic) sand, silt, peat) that vary in depth and thickness, which over multiple occurrences collectively provide a degree of confinement that lends to the development of vertical pressure gradients, as discussed in **Section 2.6**.

Comparing shallow and deep monitoring bores at the Valic Orchards shows strong evidence for confinement. Significantly greater groundwater elevation is measured at shallow screen intervals relative to the deeper piezometers. It is likely that this is due to multiple low permeability paleosols (buried ironpans), deeply buried by successive accumulations of sand (Hicks, et. al., 2001).

2.4 Recharge

2.4.1 Background Data

The proportion of rainfall that infiltrates the soils and ultimately recharges the groundwater system is relatively large, due to the high infiltration capacity of the sandy soils.

The model used in the Aupouri Aquifer Review by Lincoln Agritech (2015) suggested an annual recharge rate of 540 mm for the dune sand beneath Aupouri forest, which accounts to 43% of annual rainfall. In other groundwater studies for the region, the percentage of rainfall recharging the dune sands ranged from 10.4% to 43.7%, while for the floodplains the recharge range was 4.2% to 12.0% of annual rainfall (HydroGeo Solutions, 2000; SKM, 2007a; SKM, 2007b).

In the most recent groundwater modelling study undertaken by WWA (2017), recharge as a percentage of mean annual rainfall utilised in the model was 43% for the coastal sand zones, 38% for the weathered sand zones and 10% for the lowland plain zones. The work of WWA (2017) has been adopted in this study and is summarised in **Table 2**.

Table 2. The average annual water mass balance for each recharge zone from the SMWBM.

Recharge Zone	Groundwater Recharge	Evapo-transpiration	Runoff	Description
Coastal sand zone	43%	51%	6%	Loose sand, high infiltration capacity, low surface runoff
Weathered sand zone	38%	54%	8%	Relatively more compacted sand, high infiltration capacity, reduced surface runoff
Plain zone	10%	56%	34%	Low infiltration capacity, medium soil moisture storage, high surface runoff

2.5 Drainage

In the lower-lying farmland area, there is a man-made drainage network that typically connects to short fetch streams that discharge to the coast. The drains were installed to lower the shallow groundwater table to promote more manageable farming conditions (**Figure 3**).

Figure 3. Drainage map. (See A3 attachment at rear).

2.6 Groundwater Level Data

There are six groundwater monitoring locations within the model area (**Figure 4**). The NRC has monitoring boreholes located at Ogle drive and Paparore. The latter of these has four nested monitoring piezometers ranging in depth from 18 to 75 m below ground surface. There are four monitoring locations on the Valic Avocado Orchard. Each location features a monitoring bore drilled into the deep aquifer at a similar depth to the nearby production bore and an additional monitoring bore in the shallow aquifer. Vertical hydraulic gradients between the shallow and deep aquifer at the Valic Avocado Orchard range from 6 to 11 meters. By contrast the monitoring piezometers at Paparore measure a minimal vertical hydraulic gradient, with a slightly greater head measured at the deeper bores relative to the shallow ones.

Figure 5 shows the bore depths and mean static water level at each of the monitoring locations.

Figure 4. Location of monitoring piezometers. (See A3 attachment at rear).

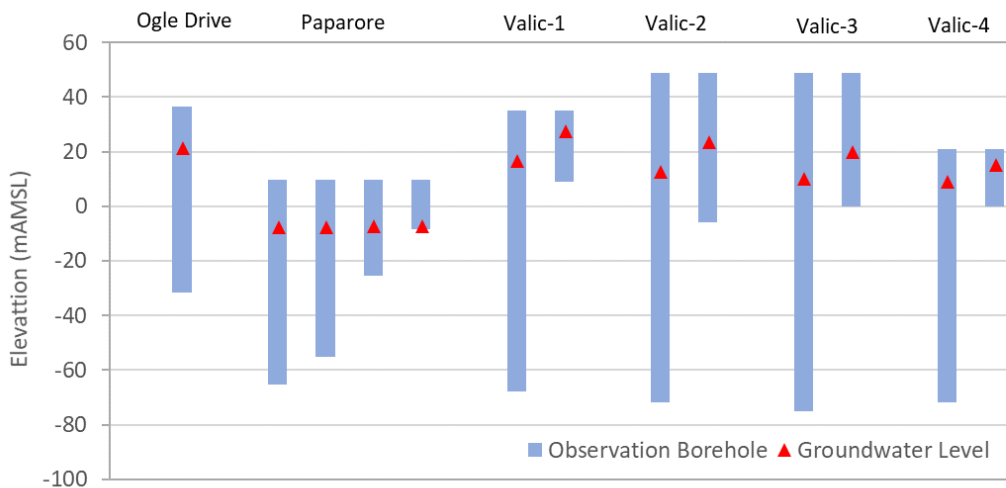


Figure 5. Mean groundwater levels of monitoring piezometers nests in the model area.

2.7 Groundwater Abstraction

Figure 6 shows the location of existing and newly proposed groundwater abstraction consents.

The current level of water allocation from the Aupouri aquifer within the Waiharara-Paparore model area is a peak daily take of 12,286 m³/day and 1.9 million m³ (Mm³) per annum from 28 groundwater take consents. This will increase to 17,545 m³/day with the proposed consents.

Figure 6. Location of existing and proposed groundwater take bores. (See A3 attachment at rear).

2.7.1 Actual Use Dataset

A historical actual use dataset is required to more accurately calibrate a groundwater model and to thereafter use the model to simulate the effects of groundwater extraction on the aquifer and surface water resources.

The SMWBM Irrigation Module was used to develop an estimate of historical actual use. The exercise combined typical irrigation scheduling (Oct - Apr) and commencement dates the consents where granted, along with an allowance for orchard development and tree growth rates to maximum water requirement. Details and results of the development of the actual use dataset are provided in **Appendix C**.

A complete dataset of historic groundwater use within the model area was not available, therefore a conservative estimate of groundwater use was generated by assuming that all active consents use were

available from the beginning of the simulation period. **Figure 7** shows the total annual volume of simulated actual use as applied in the model.

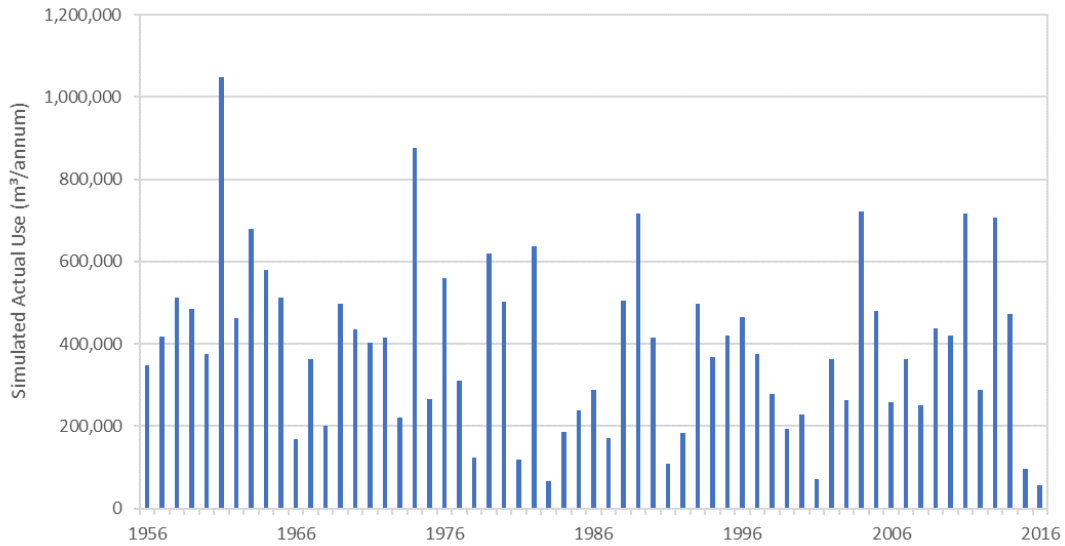


Figure 7. Simulated groundwater extraction (m³/annum partial groundwater use in 2016 due to the end of the model simulation).

3. Model Configuration

The MODFLOW Unstructured Grid (MODFLOW-USG) developed by the United States Geological Survey (USGS) was utilised within the GMS10.2 modelling platform to construct the groundwater flow model in this project. The unstructured discretisation of the model domain provides the capacity of fitting irregular boundaries into the model, and increasing the resolution to the areas of maximum interest and decreasing resolution in other areas, hence increasing the efficiency in model computation compared to the equivalent regular MODFLOW grid.

3.1 Model Domain

The model was constructed based on six layers, consisting of 29,748 active Voronoi cells (or polygons) and covers an area of 71 km². The model was discretised using different refinement schemes for major drains and bores. Finer resolution at each bore is achieved by setting the maximum radius at the refinement point of 10 m. This spatially varying discretisation approach reduces model computational time while maintaining better model resolution at the points of interest (**Figure 8**).

Figure 8. Plan view of unstructured model grid discretisation (See A3 attachment at rear).

The boundary conditions included in the model are constant head, general head, drain, and no-flow boundaries.

3.1.1 Constant Head Boundaries

The constant head boundary was assigned an elevation of 0 m AMSL along the eastern and western coastlines in Layer 1 of the model to represent the mean hydraulic head of the ocean at these locations.

3.1.2 General Head Boundaries

A general head boundary (GHB) is typically used to simulate the flow interaction between groundwater and external water sources to the model domain.

Lake Waiparera, located on the northern boundary of the model domain, was observed to have an average lake stage of 33.8 mAMSL. The groundwater level estimated from the adjacent bore was around 7 mAMSL, and this suggest that Lake Waiparera is perched above the regional groundwater system. This is also consistent with the conclusion made in the Aupouri Aquifer Review Report that the main aquifer is situated well below the surface of Lake Waiparera (Lincoln Agritech, 2015). The general head boundary was assigned to the lake to simulate lake water seeping to the underlying groundwater system, with consideration of the impedance provided by the lower-permeability lake bed sediments and/or iron pan.

The cells along the coastline from Layer 2 to 6 were also assigned with GHBs. The head values for all the cells were assigned as 0 mAMSL and the conductance value of each layer decreases with the depth to reflect the progressively increasing disconnection with the free water surface of the ocean (i.e. the impedance of flow to the ocean floor increases with depth) and also the resistance of higher-density seawater offshore. It was estimated based on model calibration that the cells along the west coast boundary had approximately one order of magnitude lower conductance than the cells along the east coast boundary.

3.1.3 No-Flow Boundaries

No-flow boundaries were assigned to cells located on the northern and southern boundaries of the model domain. Groundwater is expected to predominantly flow parallel to these boundaries from areas of high topography to low-lying coastal areas. The base of the model was also assigned a no-flow boundary on the basis that the significantly lower permeability of the basement rocks has negligible bearing on the overall flow budget of the aquifer system above.

3.1.4 Drain Boundaries

Drain boundaries were assigned in the model to simulate the groundwater discharged to the major surface drains, and to simulate the estuary that occurs along the east coast portion of the model area. The drain bed elevations were derived from the Digital Elevation Model (DEM), with a nominal depth assignment depending on locality as follows:

- **Drains in farmland** – DEM minus 2 m;
- **Drains in estuary** – DEM minus 0.5 m;
- **Drains in wetland outside of estuary** – DEM minus 2
- **Drains in estuary** – Equal to DEM elevation

The conductance value of the drains was set relatively high to reflect limited impedance to water removal (or drain functionality), to account for the significant water drainage in the farmland area and flow of water over the surface in the wetland.

3.1.5 Well Boundaries

Well points were used to represent the groundwater extraction from within the model. The model cells were assigned with negative pumping rate to represent the groundwater extraction from the model.

3.2 Simulation Package

3.2.1 Sparse Matrix Solver

The Sparse Matrix Solver (SMS) package was utilised to solve linear and non-linear equations. A maximum head change of 0.01 m between iterations was set as the model convergence criteria. Default values were used for the maximum number of iterations for linear and non-linear equations.

3.2.2 Ghost Node Correction Package

MODFLOW-USG is built on the control volume finite difference formulation, which enables the model cell to be connected to an arbitrary number of adjacent cells (Panday et al., 2013). However, this formulation will be reduced to a lower order of approximation, when the line between two connected nodes does not bisect the shared face at right angles, which will lead to errors in the simulation (Edwards, 1996). To account for this, the ghost node correction package was utilised to improve the simulation results by adding higher order correction term in the matrix solver. Ghost nodes are implicitly built into the simulation through the interpolation factors. The simulated head is systematically corrected through the ghost nodes to achieve a correct solution.

3.3 Model Layer Configuration

3.3.1 Layer Geology

The model comprises six layers that are used to represent the varying geology located in the area. The geological units assigned to each layer of the numerical model are shown in **Table 3**.

Table 3. Geological units in the model conceptualisation.

Model Layer	Stratigraphic Layer	Name	Description	Locality
1-3	1	Coastal sand	Loose coast sand, highly permeable	Western and eastern coastal strips.
	1	Weathered sand	Weathered dune sand, moderately compacted	Inland hilly or rolling country areas.
	1	Plain zone	Peaty and clayey sediments, low permeability	Inland low-lying plain areas.
4	2	Shellbed	Sand presented with shells, highly permeable	Throughout model, albeit thickness varies.
5	3	Fine sand	Old sand deposits, fine sand, moderately permeable	
6	4	Shellbed	Sand presented with more shells, highly permeable	

Model Layers 1-3 are used to represent a complex stratigraphic unit comprising alternating sands, silt, peat, clay and iron pans in a bulk sense (not discretely). It is difficult to define the sub-division in the stratigraphic layers of these deposits, hence for modelling purposes, the base of model Layer 1 was defined as an elevation of -1.5 mAMSL, while the base of model Layer 2 was defined as the base of model Layer 3 plus 22 m. Based on the 10 m vertical hydraulic gradient evident in the monitoring data at Valic-2 from the Valic-2 shallow and deep piezometers it is likely that there is a localised zone of low permeability in the subsurface in this region. This was incorporated into the model as a limited region of low conductivity relative to the surrounding material.

All model layer bases other than model Layer 1 and 2 confirm to stratigraphic interpolations as discussed in the following section.

3.3.2 Layer Elevations

The top and bottom elevation for the geological unit contacts were identified from the reliable bore logs in the area. The elevations for each unit were then interpolated using the Kriging geospatial method to generate a digital elevation surface. During interpolation, rules were applied so that geological layers did not overlap, and the surface is stratigraphically continuous.

The geometry of the basement rocks has been recognised through interpolation of the basal contact from the available bore logs in the area. **Figure 9** shows the elevation contours of the interpolated basement surface, which was assigned to base of model Layer 6 (i.e. the model bottom).

Figure 9. Basement rock elevation contours (model Layer 6 base). (See A3 attachment at rear).

Three geological cross-sections were developed from the kriged surfaces in north to south (N-S) and west to east (E-W) and directions to demonstrate the relative thickness of each geological unit. The locations of the cross-sections are shown in

Figure 10 and the cross sections themselves are shown in

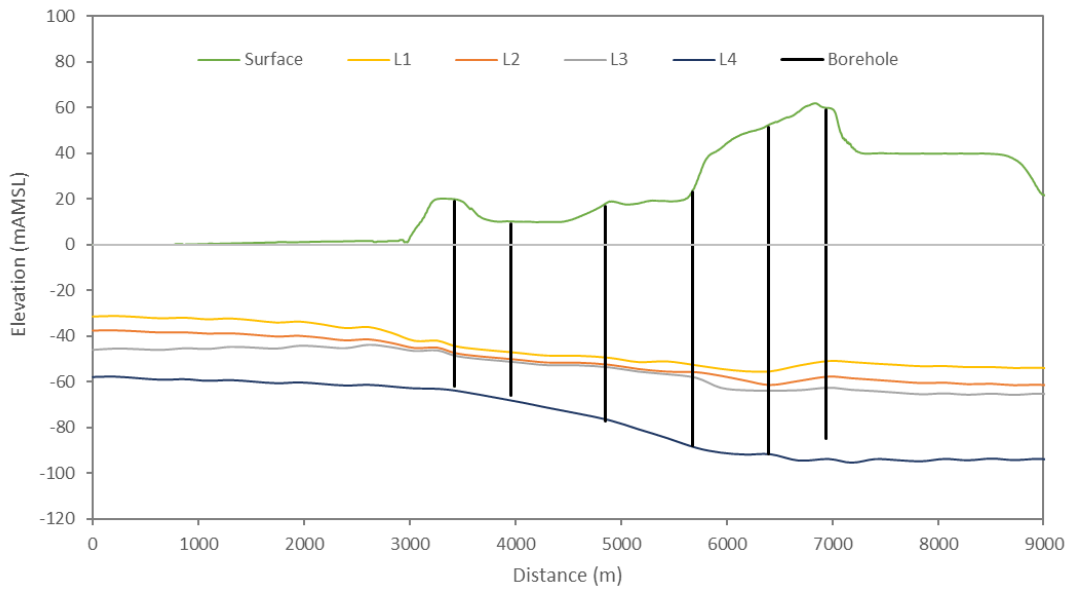
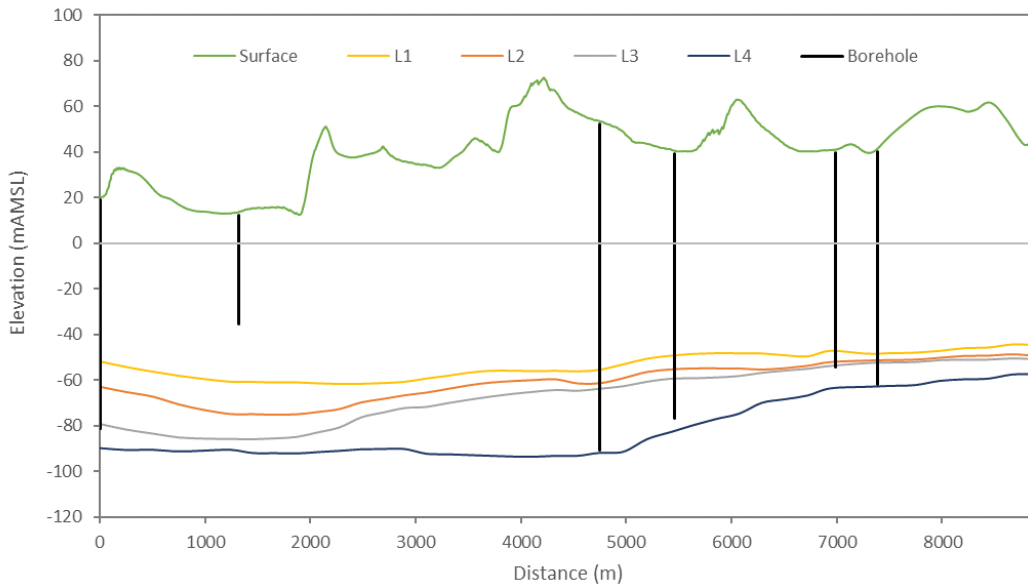


Figure 11 to

Figure 13. The constructed model grid based on the interpolated layer elevations is shown in Figure 14 .

Figure 10. Hydrogeological cross section locations. (See A3 attachment at rear).

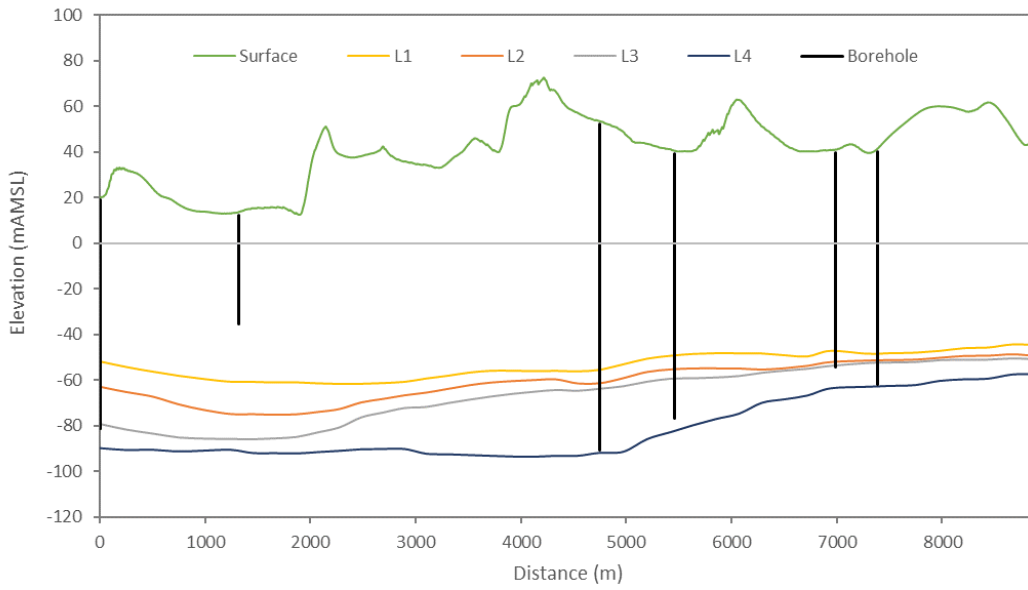


Figure 11. Interpolated cross-section at N-S (1).

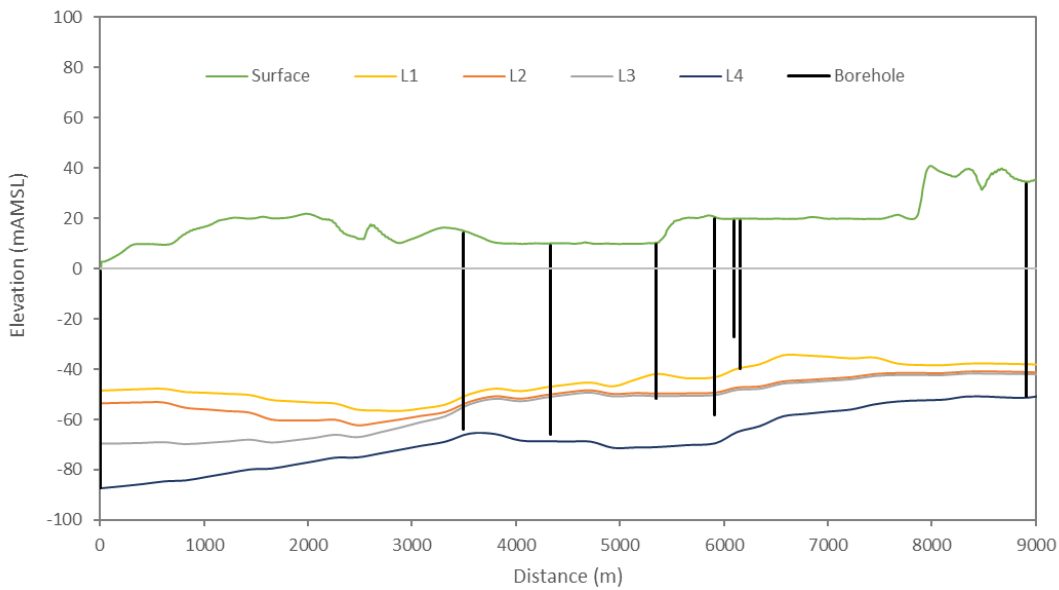


Figure 12. Interpolated cross-section at N-S (2).

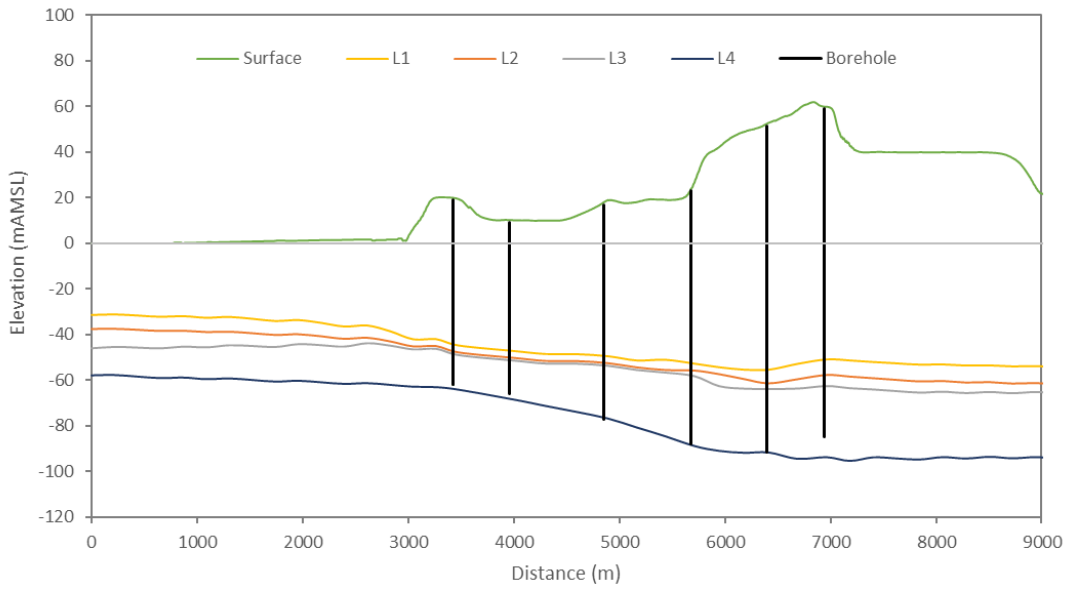


Figure 13. Interpolated cross-section at E-W (1).

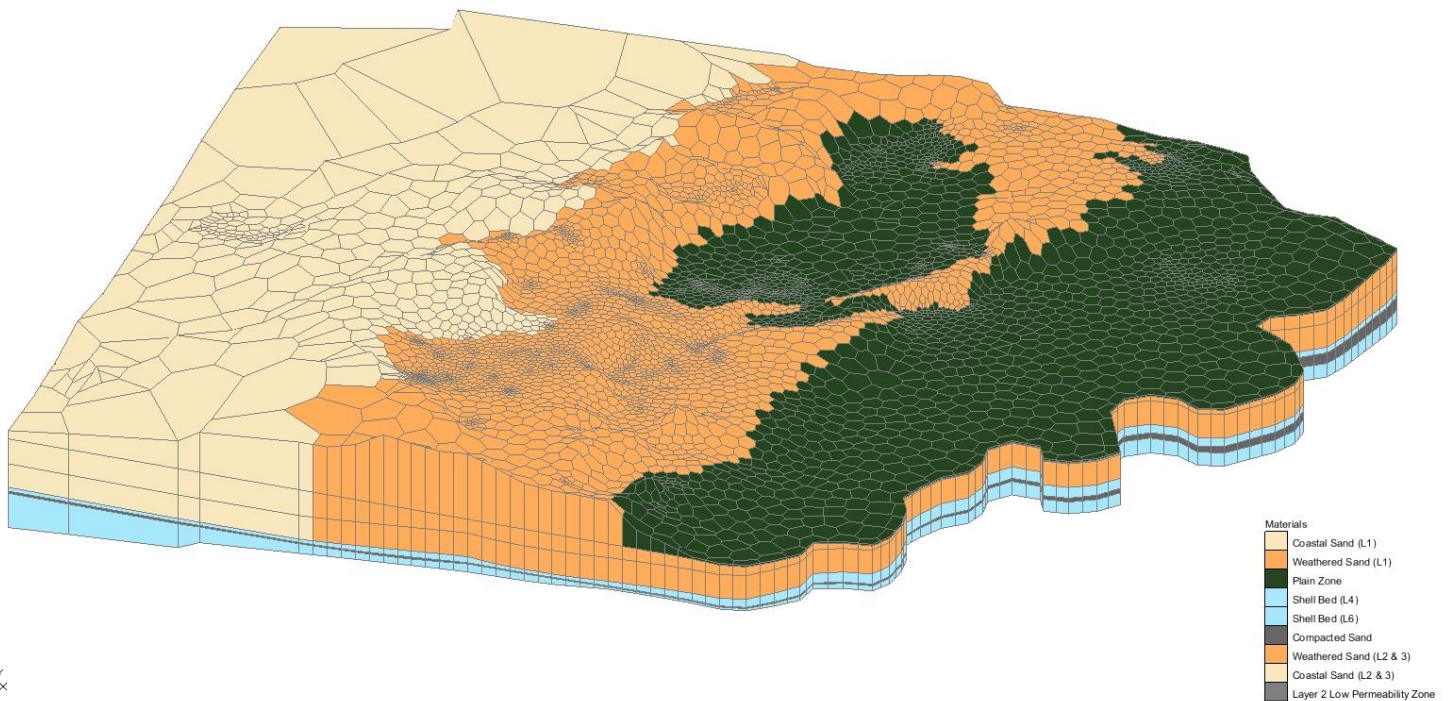


Figure 14. MODFLOW grid with vertical magnification of 10.

4. Model Calibration

The model calibration was conducted by manually changing the model hydraulic parameters to achieve an acceptable fit to measured groundwater levels. Groundwater recharge was not considered a calibration parameter.

4.1 Observation Points

The piezometers used for calibration of the model are shown in **Figure 4** and the key properties of the piezometers relevant to model calibration are summarised in **Table 4**. The piezometers are mostly nested piezometer configurations comprising adjacent standpipes installed to different depths or aquifer levels. The observation points from these piezometers were predominately located in the stratigraphic Layer 1, which meant that the vertical gradients observed in these relatively shallow piezometers would require multiple layers with vertical anisotropy to be incorporated in the model to simulate the vertical hydraulic gradients (as discussed in **Section 2.6**). To achieve this, a finer vertical discretisation of the model was required, and this was a key driver for splitting stratigraphic Layer 1 into three model layers.

To increase confidence in the groundwater level measurements used for model calibration, and thereby the model itself, an elevation survey of the 10 monitoring piezometers used for model calibration was undertaken on 6 June 2018. This survey employed a Leica TPS 1200 Total Station with vertical and horizontal accuracy of approximately ± 2 cm. The Valic production bores are located approximately 10 m from the associated monitoring bores and were assumed to be at an equal elevation. Results of this survey and other key specifications of the bores are included in **Table 4**.

Table 4. Summary of piezometers used in calibration.

Site	Piezometer Description	Surveyed Surface elevation (mAMSL)	Original Surface elevation (mAMSL)	Mean Groundwater level (mAMSL)	Standard Deviation (m)	Top of Screen Elevation (mAMSL)	Model Layer
Ogle Drive	NRC Monitoring Bore	36.35	36.39	14.90	0.32	5.15	2
Paparore	NRC Deep bore (75 mBGL)	9.74	9.67	6.88	0.664	Unknown	6
	NRC Deep bore (65 mBGL)	9.74	9.67	6.88	0.635		6
	NRC middle bore (35 mBGL)	9.74	9.67	6.46	0.264		3
	NRC Shallow bore (18 mBGL)	9.74	9.67	6.42	0.266		2
Valic-1	Shallow Monitoring Bore	29.09	35.00	21.76	0.51	12.09	1
	Deep monitoring bore	29.09	35.00	11.65	0.83	-55.41	6
	Production Bore	29.28	35.00	11.41	0.83	-63.22	6
Valic-2	Shallow Monitoring Bore	48.19	49.00	22.88	0.77	22.19	2
	Deep monitoring bore	48.19	49.00	12.24	1	-63.81	6
	Production Bore	48.19	49.00	12.06	0.85	-62.31	6
Valic-3	Shallow Monitoring Bore	49.72	49.00	20.87	2.35	39.72	6
	Deep monitoring bore	49.72	49.00	11.30	2.68	-64.28	6
	Production Bore	49.97	49.00	11.46	1.4	-63.63	1
Valic-4	Shallow Monitoring Bore	22.22	21.00	16.75	0.54	17.22	6
	Deep monitoring bore	22.21	21.00	10.77	0.55	-59.79	6
	Production Bore	22.21	21.00	10.75	0.6	-60.29	1

4.2 Steady-State Calibration

A steady-state model was developed and calibrated to validate the conceptualisation of the groundwater flow model. The objective of the calibration was to obtain approximate values of the model parameters, and to obtain initial heads for transient model simulation.

The average water levels from 17 piezometers registered on the NRC bore database were used as the calibration targets. The simulated head is plotted against the observations (**Figure 15**). The steady-state simulation has a mean head residual of -1.0 m, and root mean square error (RMSE) of 2.7 m, which is approximately 16% of the range of observations. The RMSE error has been affected by the following observations:

- Paparore (Middle and Shallow Bores) - Simulated vertical hydraulic gradient is greater than what has been observed indicating a local variation in stratigraphy not captured by the model.
- Valic-2 Shallow Monitoring Bore - Simulated vertical hydraulic gradient was less than observed data indicating the presence of a localised variation in permeability such as a hard pan. This was addressed in the transient model by adding a low permeability area in the vicinity of this bore.

If these points were ignored the RMSE is reduced to 1.8 m, representing 11% of the range of observations.

For this reason, more emphasis is placed on the transient calibration goodness of calibration fit, which is discussed in **Section 4.3**.

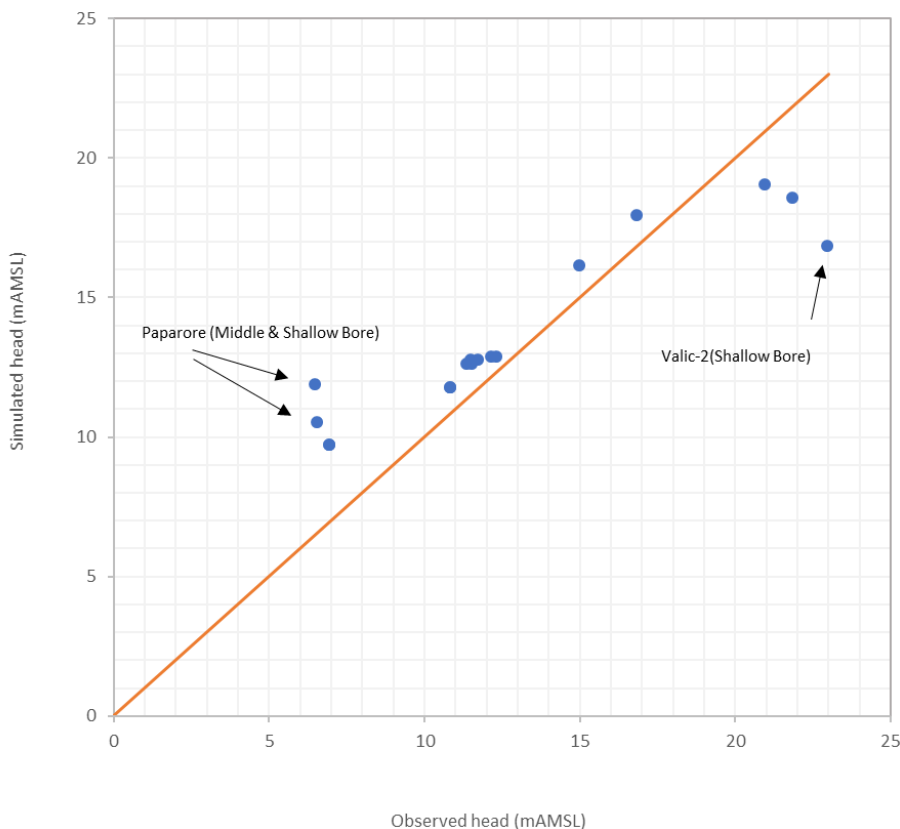


Figure 15. Simulated head versus observed head.

4.3 Transient Calibration

The model was simulated approximately 150 times to obtain a satisfactory calibration. Each transient simulation takes 10 minutes to run, and post processing of results takes 4 minutes, hence a cycle time of approximately 15 minutes for each model simulation. This cycle time enabled a significant number of calibration and sensitivity assessment runs to be undertaken.

After each run, simulated heads from the relevant model layer and cell were extracted and processed with Python code that automatically developed hydrographs, which permitted rapid comparison of simulated versus measured data.

The transient calibration setup is described in the following sections.

4.3.1 Stress Periods and Time Steps

The model was simulated in transient mode for 60 years from 1/08/1956 to 31/08/2016. The simulation was subdivided into 442 stress periods, where imposed stresses (e.g. recharge and pumping) remain constant. The number of stress periods was selected on the basis of i) temporal variation of the transient dataset values; and ii) computational time. The resulting stress period lengths ranged from 7 to 212 days. Stress periods were locked on 1 October and 30 April in each year for the start and end of the irrigation season, respectively, to ensure the irrigation demands were distributed to the correct timeframe.

Each stress period consisted of five time steps, with head and flow volume in each model cell evaluated at the end of each time step.

4.3.2 Groundwater Pumping

The estimated historical use dataset described in **Section 2.7.1** was implemented in the calibration simulations.

4.3.3 Initial Conditions

The transient model used the steady-state model heads as the starting condition. During the transient calibration process, the starting heads were re-set from periodically as parameters were updated. This enabled the starting condition to better reflect the dynamic head distribution within the model under the imposed set of stresses, and resulted in minimisation of rapid fluctuations in simulated levels and flows at the start of the simulation (i.e. increased stability).

4.3.4 Model Parameters

The calibrated model parameters are shown in **Table 5**. The calibrated model parameters are consistent with calibrated model parameters used in previous modelling (WWA 2017).

The calibrated model hydraulic conductivity for the upper and lower shellbed aquifers are 1.9×10^{-4} m/s and 2.9×10^{-4} m/s, respectively. As shown in **Table 1**, these values are within the range of horizontal hydraulic conductivity measured and modelled in the past (Layer 2 and 4) in the lower shellbed and close to the range in the upper shell bed. Similarly, for the various sand units, the calibrated model values range from 1.4×10^{-5} m/s to 6.9×10^{-5} m/s, which is consistent with the range in previously documented values shown in **Table 1**.

Table 5. Calibrated model parameters.

Model Geological Units	Model Layer	Kx		Vertical Anisotropy	Sy	Ss
		(m/d)	(m/s)	(-)	(-)	(m-1)
Coastal sand	1	3.7	4.28E-05	30	0.3	-
Weathered sand	1	1.2	1.39E-05	45	0.25	-
Plain zone	1	0.5	5.79E-06	15	0.05	-
Coastal sand	2&3	2.3	2.66E-05	40	-	7.00E-04
Weathered sand	2&3	0.6	6.94E-06	60	-	1.60E-04
Low Permeability Area	2	0.3	3.47E-06	150	-	1.60E-04
Shellbed	4	16.0	1.85E-04	1	-	7.00E-05
Sand	5	0.5	5.79E-06	60	-	2.00E-04
Shellbed	6	25.0	2.89E-04	1	-	7.00E-05

4.4 Calibrated Model Output

4.4.1 Groundwater Levels

As previously stated in **Section 2.6**, groundwater levels recorded within 17 NRC monitoring piezometers were used to calibrate the transient groundwater model. **Appendix D** provides hydrographs and water level maps of simulated groundwater levels plotted against observed data for comparison purposes, and an assessment and commentary on the goodness of fit for each hydrograph is provided in **Table 6**.

Table 6. Comparative assessment summary of the goodness of fit between simulated and observed groundwater heads.

Site	Piezometer	Model Layer	Location	Fit		Comments
				Qualitative	RMSE	
Ogle Drive	NRC Monitoring Bore	2	Interior of model area near boundary of weathered sand and coastal sand	Excellent	0.3	Strong correlation between simulated and measured data.
Paparore	NRC Deep bore (75 mBGL)	6	East -model interior	Moderate	2.6	Simulated water levels are significantly lower than measured. Oscillations reflect measured data.
	NRC Deep bore (65 mBGL)	6		Moderate	2.6	
	NRC middle bore (35 mBGL)	3		Moderate	3.8	
	NRC Shallow bore (18 mBGL)	2		Moderate	5.2	
Valic-1	Shallow Monitoring Bore	1	Centre of model area-near coastal sand	Moderate	1.2	Simulation in deep aquifer is in the range of measured data. Shallow aquifer is generally low.
	Deep monitoring bore	6		Good	1.0	
	Production Bore	6		Good	1.2	

Site	Piezometer	Model Layer	Location	Fit		Comments
				Qualitative	RMSE	
Valic-2	Shallow Monitoring Bore	2	Centre of model area-near coastal sand	Poor	6.1	Vertical hydraulic gradient is not matched by simulation. Good correlation in deep aquifer.
	Deep monitoring bore	6		Good	1.2	
	Production Bore	6		Good	1.0	
Valic-3	Shallow Monitoring Bore	6	Interior of model area-weathered sand	Moderate-Good	1.3	Simulated water levels are in the range of measured data. Temporal trends are inconsistent.
	Deep monitoring bore	6		Good	2.0	
	Production Bore	1		Good	2.2	
Valic-4	Shallow Monitoring Bore	6	Center of model area-near plain zone	Moderate	1.7	Simulation is high in both shallow and deep aquifer but generally within 1 m in the latter. Good match for simulated oscillations in the deep aquifer
	Deep monitoring bore	6		Moderate-Good	0.9	
	Production Bore	1		Moderate-Good	0.9	

The mean residual head is -1.6 m and the geometric mean of the RMSE is 2.43 m, which is 9% of the observed range in groundwater head (26.8 m). A simulated RMSE of less than 10% of the measured range is considered a good calibration. Measured data at all deep aquifer bores at the Valic locations and at Ogle Drive were well represented by the model as evident in the hydrographs provided in **Appendix D**. Simulated groundwater levels at the deep bores in the Valic orchards are generally within 1 meter of measured values except Valic-3 where there is a greater discrepancy in earlier data; however, the last 5 years of the measured data set is similar to simulation results.

The RMSE stated above reflects the difficulty that was encountered in simulating measured groundwater levels in the shallow aquifer at the Paparore and Valic-2 bore. The monitoring piezometer at Paparore is significantly oversimulated with measured groundwater levels typically 5 m above measured levels at the shallow piezometer (18 mBGL) and nearly four meters greater than observed levels at the middle monitoring piezometer (35 mBGL) while the deeper piezometers were approximately 2.5 m above observations. The vertical hydraulic gradient was not well simulated indicating that a localised variation in permeability, reflecting the complex stratigraphy in the model area, may impede model calibration at this location.

The vertical hydraulic gradient is also not well captured at the Valic-2 location. The low permeability zone applied in Layer 2 of the model improved this somewhat but it remains likely that the conceptual model does not capture some of the geologic complexity this area. If the shallow bores at Paparore and Valic-2 are excluded the model RMSE becomes 1.44 m (5% of the observed range) and mean residual head becomes -0.05 m.

4.4.2 Model Flow Budget

Table 7 provides the long-term average water budget for the transient calibration model. The main input to the model is groundwater recharge at 75% of the total inflow. The predominant discharge component from the model are the subsurface coastal discharges, which are comprised of the constant head in Layer 1 (35%) and the GHB in Layer 2 to 6 (13%). Surface water discharges in the form of drains and wetlands account for 24% of the model water budget.

Table 7. Average daily mass balance for 60-year simulation from 1/08/1956 to 31/08/2016.

Mass balance	Components	Flow (m ³ /d)	Percentage of Flow (%)
Inflow	Storage	20,335	23.6
	CH	0	0.0
	Recharge	64,906	75.4
	Lake Waiparera	788	0.9
	Total inflow	86,029	100
Outflow	Storage	20,833	24.2
	Shallow Coastal Discharge (CH)	29,796	34.6
	Wells	3,574	4.2
	Drains/Wetlands (DC)	20,402	23.7
	Deep Coastal Discharge (GHB)	11,438	13.3
	Total outflow	86,043	100
Percentage discrepancy		-0.02%	

5. Predictive Simulations

5.1 Scenario Setup

The numerical groundwater model was developed to assess the effect of various groundwater abstraction rates on the local aquifer. A transient pumping dataset for each bore was developed using the simulated irrigation demand time series described in **Appendix C**. This assessment was expanded to include a sensitivity analysis where the permeability of model Layer 2 was reduced.

This was undertaken because the calibrated groundwater model has an acknowledged limitation with regard to over simulation of vertical leakage due to partial absence of the multi-layered but irregular and discontinuous iron pans and other low permeability horizons within the sedimentary sequence, which act as a flow barrier between the deeper groundwater system and the surface drains and wetlands. As a result, the model exaggerates the effects of the proposed abstraction on the groundwater levels in the shallow aquifer and at the surface. Conversely, the model under-predicts the local-scale drawdown in the deeper aquifer.

To investigate model uncertainty with regard to simulated drawdown in the deeper shellbed layer, a scenario was devised with permeability modified in Layer 2, which is the depth range where iron pans and peats layers prevail. Horizontal hydraulic conductivity of Layer 2 was decreased to 1×10^{-9} m/s in both the coastal sand and weathered sand regions, with vertical anisotropy remaining similar at a factor of 50. Boundary and source/sink conditions remained the same as in the baseline model. The model was not calibrated to the conditions applied in Scenarios 3, therefore Scenario 3 results are only referenced to illustrate relative (rather than absolute) changes in groundwater level and water budget.

Stress periods in the predictive scenarios were the same as in the transient calibration simulations described in **Section 4.3.1**. In effect, the climatic conditions of the last 60-years have been utilised to simulate the next 60 years.

The three predictive model scenarios can be summarized as follows:

- **Scenario 1: Basecase** – the calibration model which includes the current 27 consented groundwater takes at a peak abstraction rate of 11,620 m³/day.
- **Scenario 2: Proposed Extraction** – includes current and proposed groundwater extraction totalling a combined peak rate of 16,602 m³/day. This was applied through 4 new groundwater take bores in addition to the 27 existing bores.
- **Scenario 3: Low Permeability-Proposed Extraction** – Groundwater extraction is the same as in Scenario 2 with horizontal hydraulic conductivity of Layer 2 was decreased to 1×10^{-9} m/s in both the coastal sands and weathered sand regions to simulate a hard pan extending over the model area.

5.2 Model Results

Based on the rainfall record and simulated groundwater response in the base model, the end time of a dry period with maximum water use was selected for impact analysis. The selected date was April 30, 2010, corresponding to the lowest water levels over the simulation period.

5.2.1 Mass Balance

A comparison of the average flow budget at the end of the 2009-2010 irrigation season (peak drawdown) for all three scenarios is provided in **Table 8**.

Table 8. Average flow budget for April 30, 2010 (peak drawdown).

Mass balance	Components	Baseline		Scenario 2: Proposed Extraction		S3: Low permeability-increased pumping	
		Flow (m ³ /d)	Percentage of Flow (%)	Flow (m ³ /d)	Percentage of Flow (%)	Flow (m ³ /d)	Percentage of Flow (%)
Inflow	Storage	58,874	89.7	60,873	90.0	49,803	88.0
	CH	0	0.0	0	0.0	7	0.0
	Recharge	6,000	9.1	6,000	8.9	6,000	10.6
	Lake Waiparera	785	1.2	794	1.2	801	1.4
	Total inflow	65,659	100	67,667	100	56,610	100
Outflow	Storage	0	0.0	0	0.0	0	0.0
	Shallow Coastal Discharge (CH)	29,815	45.4	29,376	43.4	5,407	9.6
	Wells	10,339	15.7	14,766	21.8	14,766	26.1
	Drains/Wetlands (DC)	14,737	22.4	9,606	14.2	27,630	48.8
	Cross Boundary Groundwater Flow (DC)	0	0.0	3,618	5.3	6,392	11.3
	Deep Coastal Discharge (GHB)	10,767	16.4	10,302	15.2	2,417	4.3
	Total outflow	65,658	100	67,668	100	56,612	100
Percentage discrepancy		0.00%		0.00%		0.00%	

Note: CH = constant head; GHB = general head boundary; DC = drain cells

The peak of groundwater extraction proposed in Scenario 2 is estimated to account for an additional 6.1% of the total water budget going to irrigation for April 30, 2010 (corresponding to the lowest water levels of the simulation period), the increase in water taken for irrigation accounts for 1.6% of the total water budget. The abstraction reduces coastal discharges (CH/GHB) and surface drainage (DC) while slightly increasing accession from storage.

Drawdown from increased pumping in the adjacent Motutangi region immediately north of the model area is estimated to induce cross boundary groundwater flow out of the model domain amounting to 5.3% of the groundwater budget for the time period of interest.

Lake Waiparera is hydraulically indirectly connected (or partially disconnected) to the regional groundwater system, as evidenced by water observed to overflow the surface of the lake by local residents. Hence, the water discharged from the lake to the groundwater system is a small component of the overall groundwater budget (1.2%).

Scenario 3 was also evaluated for its impact of the simulated water budget during peak drawdown. The low permeability layer applied reduced leakage into the deep aquifer and thereby increased discharge to surface water via drains and wetlands as evidenced by surface drainage increasing from 22% of model outflows in the Baseline Model to 49% in Scenario 3. Shallow coastal drainage in Scenario 3 was predicted to decrease from 45% to 10% of the model outflows relative to the Baseline Model, with water discharging into upgradient drains and wetlands rather than at the coast.

Deep groundwater discharge was also predicted to decrease from 16% to 4% in Scenario 3 as groundwater levels decline in the deep aquifer, a function of the lower permeability as well as the increased groundwater extraction. Cross boundary groundwater flow resulting from cumulative effects from groundwater takes in the Motutangi region increased to 11% of the predicted outflow due to drawdown increasing the hydraulic gradient.

5.2.2 Drain Flows

An analysis of the impact on flows including discharge to both farm drains and wetlands was undertaken for low-flow situations. The annual minima in daily flow was obtained from the global flow budget for all drain boundary cells combined for each time step exported from the model. Annual recurrence intervals were calculated from this table of data for each scenario, and the resulting data is presented in **Table 9** and **Figure 16**.

A comparison of the proposed groundwater takes (Scenario 2) against the base case indicates that the mean annual (1-year) low flow has potential to be reduced by a maximum of 4% and the 5-year low flow by 9%. However, as stated earlier, we consider the model to exaggerate groundwater level reduction in the shallow aquifer and at the surface because of the lack of hard pans in the model. In this regard, these values should be treated as conservative upper estimates.

It is evident in these results that the variation in annual minimum discharge from groundwater to surface water over a range of drought severities (i.e. annual to 100-year recurrence interval) is not significant (30% reduction) and that with the proposed pumping this reduced by a further maximum of 10% during a 100-year drought event.

Table 9. Low-flow analysis of surface discharge and percentage reduction in flow from base case.

Recurrence Interval	Scenario 1: Baseline	Scenario 2: Proposed GW Extraction	
		(L/s)	(%)
(years)	(L/s)	(L/s)	(%)
1	218	209	-4%
2	183	170	-7%
5	171	155	-9%
10	165	149	-9%
25	158	143	-9%
50	158	142	-10%
100	156	141	-10%

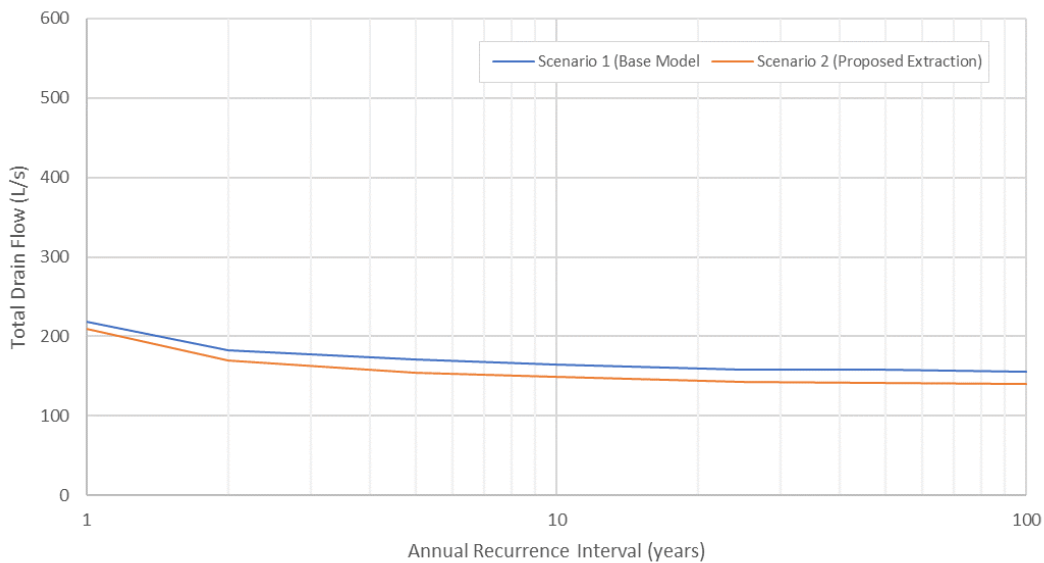


Figure 16. Surface drainage low flow analysis for model predictive scenarios.

5.2.3 Water Level Impacts

Three locations were assessed for each scenario for the shallow and deep aquifer, respectively, to evaluate the relative impacts of the scenario conditions on ambient water levels across the model area (

Figure 17). The relative responses for North, Centre, and South locations are shown in Figure 18 to Figure 20, respectively. These graphs are provided to give a sense of the comparative differences in water levels expected at different depths in the aquifer from the scale of pumping utilised in the model scenarios as well as sensitivity of simulated water levels in the upper and lower aquifer to reduced permeability.

Figure 17. Locations for scenario groundwater level analysis (See A3 attachment at rear).

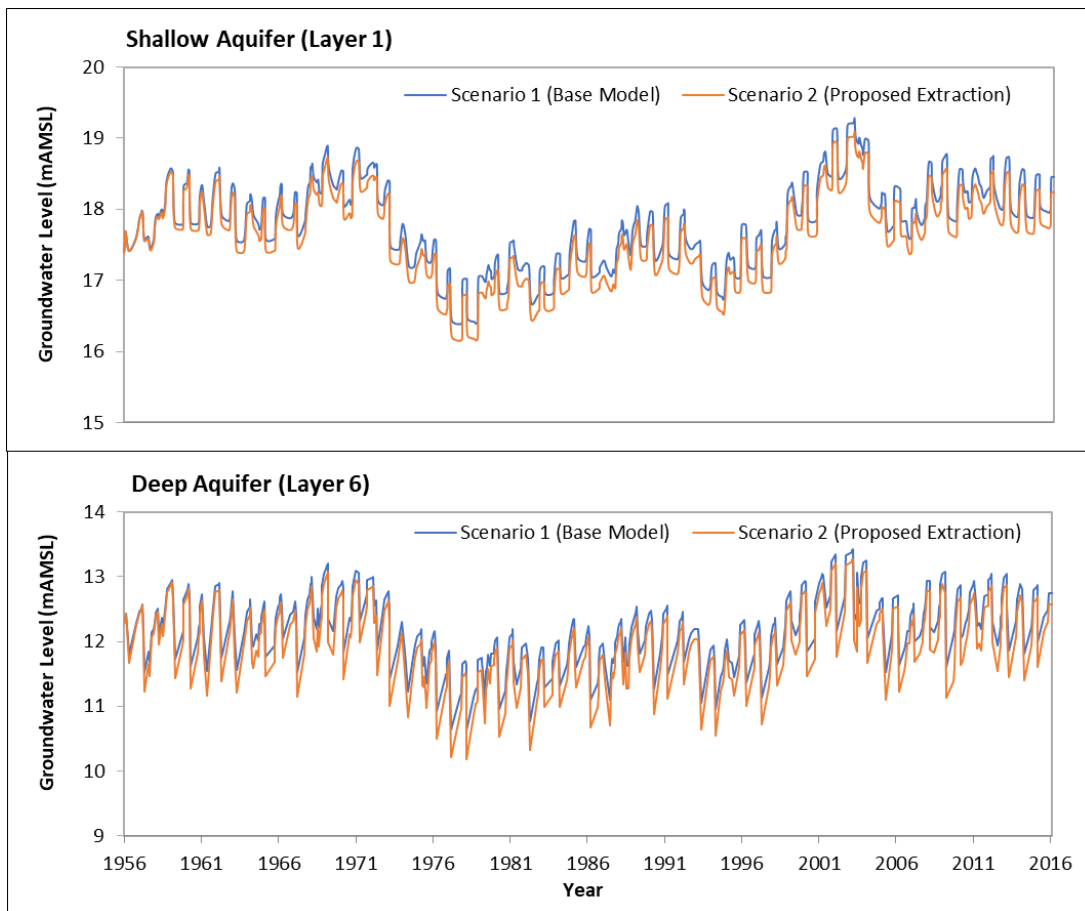


Figure 18. Groundwater level hydrographs for North reference location

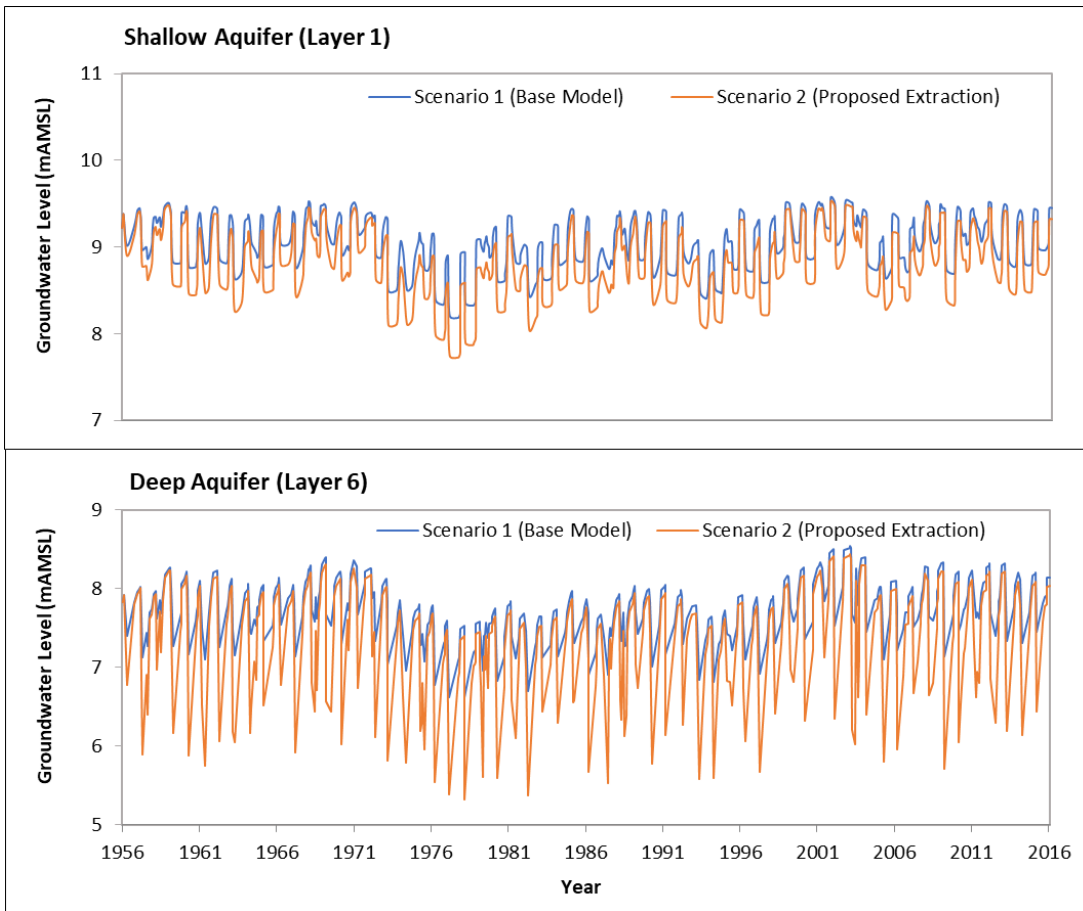


Figure 19. Groundwater level hydrographs for Centre reference location.

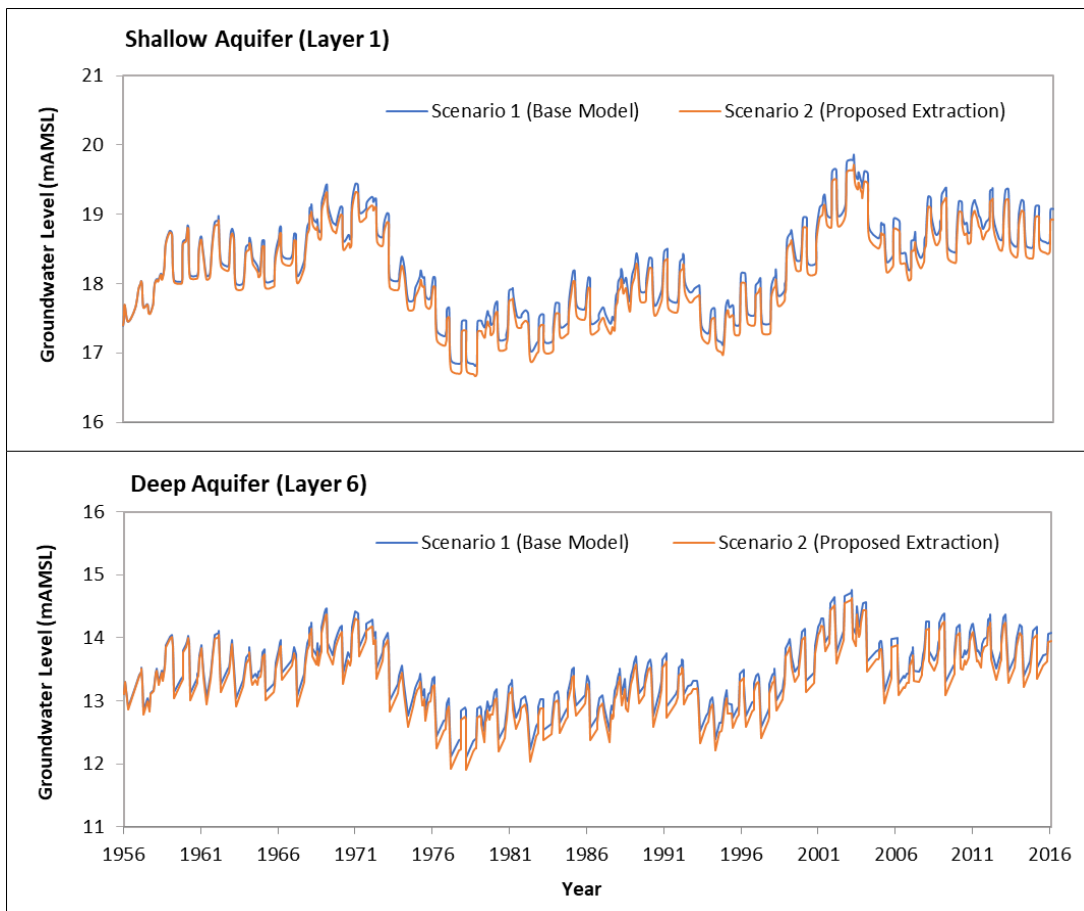


Figure 20. Groundwater level hydrographs for South reference location

The simulated impact of increased pumping is greater in the Centre reference location than in the North or South reference locations because of its proximity to the added production bores. Groundwater levels in the deep aquifer are predicted to decline at the centre reference location by approximately 1.5 m when peak irrigation occurs, while only declining 0.3 to 0.4 m in the shallow aquifer. The difference in drawdown between the two aquifers is due to pumping occurring in the deep aquifer.

When there is no irrigation, groundwater levels are approximately equal between the two scenarios. The predicted drawdown at the North reference location reflects the cumulative impact of increased pumping in the Motutangi area north of the model boundary as well as pumping from within the model area. The overall decline in groundwater level is up to 0.7 m in the deep aquifer and approximately 0.2 m in the shallow aquifer. The impact of increased groundwater pumping in the southern portion of the model area is predicted to be minimal in both aquifers (**Figure 20**).

5.2.4 Drawdown Effects

The simulated April 30, 2010 groundwater level for Scenario 2 and Scenario 3 was subtracted from the head simulated at the corresponding time from the Baseline Model in the case of Scenario 2, and a revised version of the Baseline model with low permeability in Layer 2 for Scenario 3, to produce regional drawdown maps (**Figure 21 - Figure 23**). The resulting drawdown predictions are used to evaluate the potential impact proposed pumping under both scenario conditions.

Areas outside of the model boundary were considered with regard to the cumulative effect of groundwater pumping in the Waiharara-Paparore model area and adjacent areas. It was determined that drawdown from the Motutangi region to the north of the model reported in WWA (2017) would need to be considered, while

drawdown from production bores south of the model area was considered unlikely to extend as far as the model boundary based on the conclusions of a groundwater assessment for Awanui region to the south of the Waiharara-Paparore (SKM, 2007a).

To account for the cumulative effect of groundwater pumping in the Motutangi area, drawdown was calculated from the initial model results for Scenario 2 and Scenario 3 and subsequently subtracted from the resulting groundwater head along the northern model boundary. The resulting elevations were applied in the model as a boundary condition limiting groundwater elevations along the northern model boundary.

The following paragraphs discuss the results for the various features.

Deep aquifer

In Scenario 2 the maximum drawdown was 3.2 m at the proposed Tiri Avocado pumping locations and the extent of drawdown (taken as the 0.6 m drawdown contour) was approximately 2.3 km from the peak drawdown location, as shown in **Figure 21**. In Scenario 3 the low permeability of model Layer 2 limited recharge thereby magnifying the impact of pumping on groundwater levels. The maximum drawdown predicted in Scenario 3 was 4.2 m at the pumping locations, while the extent of drawdown from the peak location ranged from approximately 4 km to northeast to 6 km to the south. The influence of drawdown in the adjacent Motutangi area is also more apparent in Scenario 3 relative to Scenario 2 with the drawdown profile stretching laterally toward the northern model boundary rather than centring on the new groundwater takes (**Figure 22**).

Figure 21. Simulated drawdown of deep aquifer (Scenario 2). (See A3 attachment at rear).

Figure 22. Simulated drawdown of deep aquifer (Scenario 3). (See A3 attachment at rear).

Shallow aquifer

The shallow aquifer is less affected by the pumping at the deep aquifer, however, there is drawdown simulated for the proposed extraction scenario (Scenario 2) relative to the Baseline Model. The maximum predicted drawdown in the shallow aquifer is 0.5 m. Greater drawdown was predicted in the vicinity of the new groundwater takes, however the location of agricultural drains influenced the distribution of drawdown by limiting water levels equally in both scenarios (**Figure 23**). Shallow aquifer drawdown due to increased groundwater pumping in Scenario 3 was negligible because of the disconnection of the upper and lower portions of the aquifer.

Figure 23. Simulated drawdown of shallow aquifer (Scenario 2). (See A3 attachment at rear).

Existing bores

The drawdown induced by the groundwater take utilised in each scenario was calculated and plotted similarly at 27 existing bores as a boxplot, with the maximum and minimum drawdown shown in

Figure 24.

The drawdown at the existing bores predicted in Scenario 2 is largely affected by their distance to the proposed new groundwater take locations. At the driest condition (30/04/2010), the simulated drawdown in Scenario 2 ranges between 0.18 m to 1.16 m. The maximum drawdown of 1.16 m was predicted at the Valic-3 bore, 600 m west of the proposed Valic-4 bore, and the minimum drawdown of 0.18 m was predicted at the DC & MA Olsen bore near the southern model boundary.

For the same date in Scenario 3 simulated drawdown ranged from 0.83 m to 2.24 m with greater drawdown predicted to the north of the new groundwater takes compared to bores to the south of the new groundwater

takes due to the cumulative influence of additional pumping combined with lack of recharge. The maximum drawdown was predicted at the Bell bore approximately 500 m northeast of the proposed Tiri Avocado bore, and the minimum drawdown was predicted at the DC & MA Olsen bore.

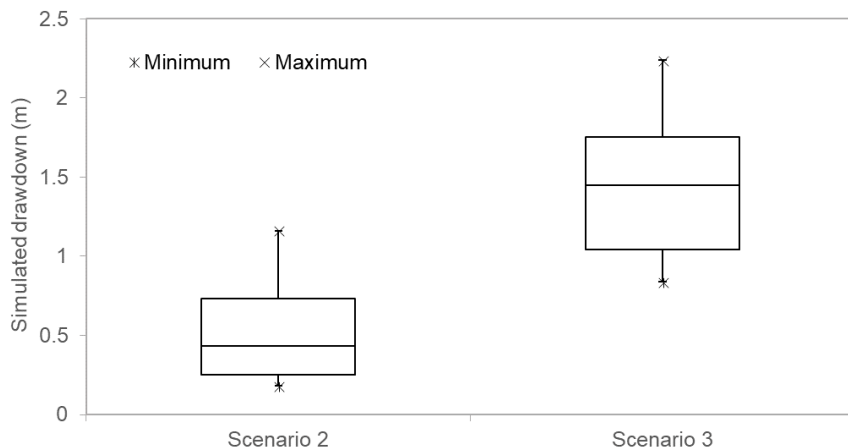


Figure 24. Drawdown observed at existing bores at the observation time step for each scenario.

5.2.5 Saltwater Intrusion

Saltwater intrusion under the hydrogeological conditions in the Waiharara-Paparore region, and specifically into the shellbed aquifer is best evaluated using the method of *Lateral Migration Analysis*. Lateral migration along the aquifer/bedrock interface considers the material under the aquifer impermeable where inland migration of salinity occurs via the permeable sediments along the lower boundary of the aquifer. This mechanism assumes that the pressure at the coastal margin is relevant to maintaining an offshore position of the saline interface.

The shellbed aquifer in the Waiharara-Paparore region underlain by relatively impermeable basement rock is well represented by this conceptual approach.

5.2.5.1 Lateral Migration Analysis

Based on the estimated depth to the basement rock at the coastal margins, the Ghyben-Herzberg relation was used to back-calculate the minimum hydraulic head required to maintain the saline interface below the shellbed aquifer (i.e. the lateral migration “Trigger Level”). This calculation was performed at selected points at approximately 200 and 500 m intervals along the coastal margins on the east and west model boundaries, respectively. Greater point density was used for the east coast because the coastline is in closer proximity to developed areas and active groundwater pumping. The simulated groundwater levels for Layer 6 from each scenario were extracted for these points.

Saltwater intrusion is not an instantaneous response to the lowered water table - it is a gradual process requiring prolonged reduction in groundwater level below a critical level to initiate the landward migration of the saline interface. A 90-day rolling average (RA) was calculated from the simulated groundwater level to reflect this slow process. The simulated groundwater levels were then compared against the Trigger Level at the model times 10/06/1973 and 1/05/1978, which represent an average and lowest groundwater level drought condition, respectively.

The location of the points is shown in **Figure 25**. The points were selected to provide an adequate coverage with a spacing of approximately 200 m on the east coast and 500 m on the west coast. Greater density of analysis points was applied on the east coast because of closer proximity to current and potential development areas.

Figure 25. Location of the selected points for lateral migration analysis (see A3 attachment at rear).

The hydraulic heads in the deep shellbed at the two selected time steps (01/05/1978 and 10/06/1973) in Scenario 2 are on average approximately 3.7 m and 4.2 m greater than the pressure required to maintain the saline interface below the shellbed aquifer at the selected points.

The 90-day average minimum groundwater level over the entire simulation time (1956-2017) for reference locations along the east coast are shown in **Figure 26** and for the west coast are shown in **Figure 27**. This shows that the simulated minimum groundwater levels are greater than the head required to maintain the saline interface below the deep shellbed aquifer for the nearly the entire model boundary.

At reference points 13 and 14, located on the margin of the estuary to the south of the Waiparera Stream, there appears to be potential for saline intrusion under baseline conditions as well as with the additional groundwater extraction proposed. There is minimal difference in predicted groundwater level between the two scenarios.

It should be noted that this area is located in an estuary and is not considered to have potential for agricultural development. The closest bore to this area is Ellbury Holdings, situated approximately 150 m west of reference point 3. At its lowest point in the simulation period, 90-day running average for groundwater head at reference point 3 is 1.3 m above the minimum head required to avert saline intrusion. It can be concluded that saltwater inland migration along the basement contact is unlikely to increase in response to the proposed groundwater extraction and is unlikely to adversely impact any wells that are currently operating.

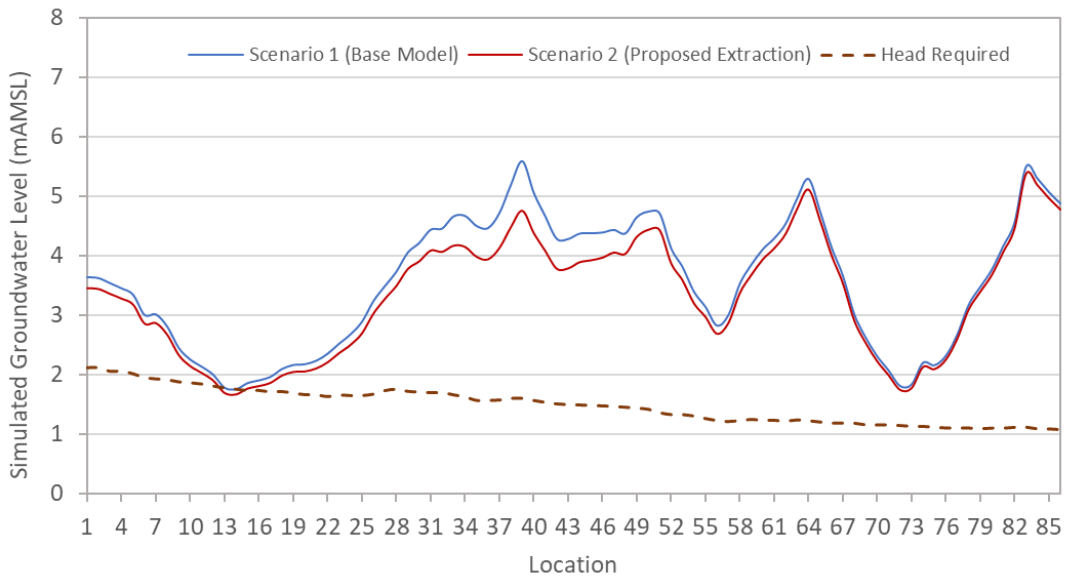


Figure 26. Simulated minimum groundwater level between 1956 and 2016 in Layer 6 (East Coast, NE to SE).

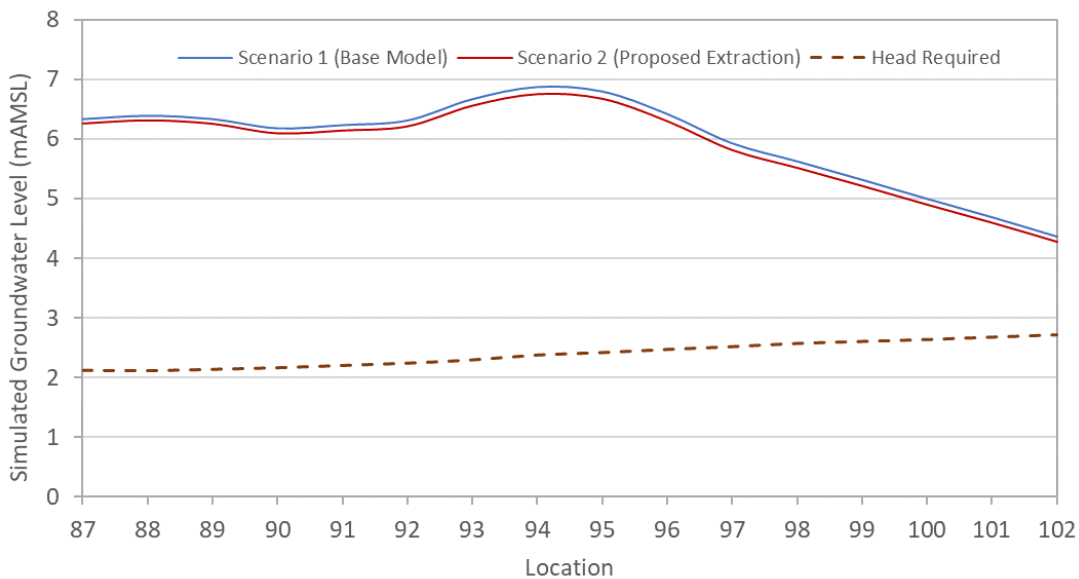


Figure 27. Simulated minimum groundwater level between 1956 and 2016 in Layer 6 (West Coast, SW to NW).

As noted above, the simulated groundwater level at coastal points 13 and 14 periodically falls below the trigger level. In **Figure 28** the 90-day RA groundwater head for Scenario 1 and Scenario 2 is compared to the minimum head required to deter saltwater intrusion, which is approximately 1.78 mAMSL at this location. It is apparent that the Layer 6 groundwater head is typically above the minimum head threshold while occasionally (12 times in 60 years – 5 year recurrence interval) falling below when it approaches its annual minima during dry years.

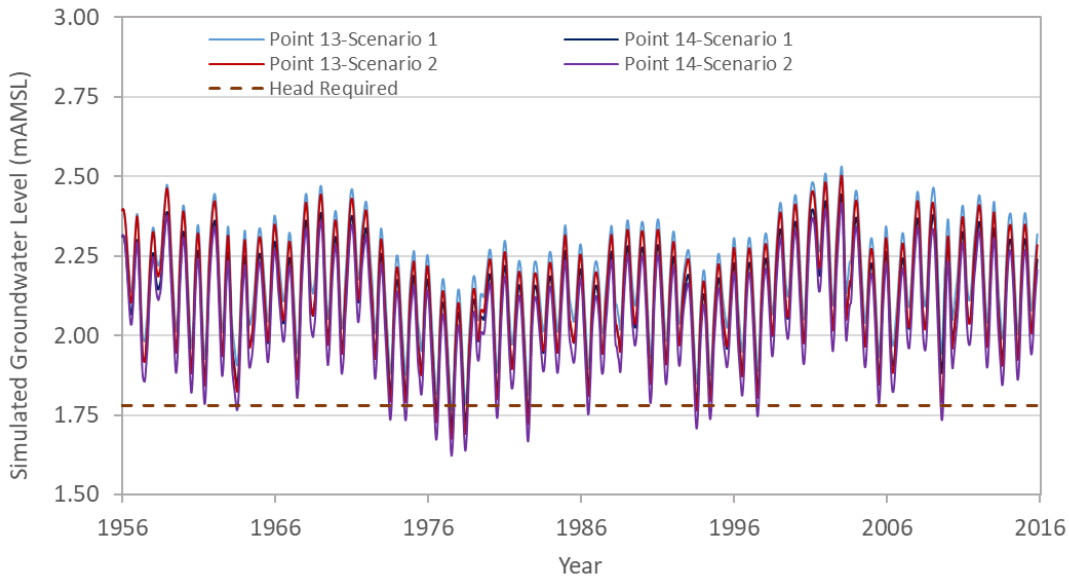


Figure 28. Simulated groundwater level in Layer 6 at coastal point 11.

Considering the future development and its adjacency to the coastline, it is recommended to establish a sentinel piezometer at point 38 shown in **Figure 25**-to effectively monitor the trigger level of saltwater intrusion in an area where such an occurrence would pose significant risk for currently operating farms.

6. Conclusions

A numerical groundwater flow model was developed to determine the potential impact from the proposed groundwater abstraction on the regional aquifer system and the hydrological condition of relevant surface water. In particular, the model was used to define the potential impact from seasonal pumping on the aquifer system water budget, aquifer groundwater levels, surface water drain flows, and the position of the saltwater/fresh water interface.

Water Budget

At the time of peak irrigation total groundwater abstraction under current conditions accounts for 15.7% of the groundwater budget, increasing to 21.8% of the water budget with the proposed groundwater takes, which represents an increase of 6.1%. The increase in groundwater abstraction is balanced by an 8.2% decrease in discharge to drains and decreasing coastal discharge.

Change in Water Levels

The proposed abstraction has potential to change groundwater levels in both the deep and the shallow aquifer, particularly during dry times, but the aquifers respond quickly to wetter climate following the irrigation season.

Change in ambient water level was evaluated at three reference locations for 30/04/2010, corresponding to the heaviest irrigation season in the simulation period. At this time, the proposed abstraction induced a maximum of 1.5 m and 0.4 m decline in groundwater head in the deep and the shallow aquifer, respectively. Greater declines were predicted in the northern portion of the model due to the cumulative effect of pumping in the Motutangi area north of the model boundary.

Predicted drawdown at existing bores was primarily governed by their distance to the proposed groundwater takes. At the driest time (30/04/2010), the simulated drawdown at neighbouring bores ranged between 0.2 to 1.2 m with the new groundwater takes applied to the simulation. A drawdown of 0.6 m was predicted approximately 2.3 kilometres from the new groundwater takes under baseline model parameters.

As the base model setup has not comprehensively captured the existence of hard pan layers in the shallow aquifers and thus the degree of confinement of the deeper shellbed aquifer, drawdown in the deeper aquifer is under-estimated. A sensitivity analysis that involved increasing confinement of the deep aquifer in the model indicated a maximum drawdown ranging from 0.8 to 2.2 m at neighbouring bores under the proposed abstraction. This is likely to be the upper bound for drawdown in the deeper shellbed aquifer while shallow aquifer levels were not impacted under these conditions. With the decreased permeability a drawdown of 0.6 m was predicted approximately 4 kilometres to the northeast and approximately 6 kilometres to the south of the peak drawdown location. There was a notable increase in cumulative impact from drawdown in the Motutangi area. Absolute water levels from this scenario were not considered in the assessment of low permeability because the model was not calibrated to these conditions

Saline Interface

While the model shows a significant potential rise in the level of the saline interface with the proposed abstractions compared to the base model, the saline interface on the east coast remains safely below the sedimentary (shellbed) aquifer in areas where agricultural development has been established adjacent to the coastline.

The area of concern for saline intrusion as identified by the model is at the mouth of the Waiparera Stream, near the northeast corner of the model area. It is likely that this area periodically has a saltwater interface that migrates inland under particularly dry condition; however, it is not an area that is suitable for agricultural development as it is on the margin of the estuary. Based on model result it is unlikely that the proposed groundwater takes will increase the inland migration of saline water along the shellbed aquifer/bedrock interface; however, it is recommended to install a sentinel piezometer near reference point 38 because this is an area where there are established farms near the coastline.

Lake Waiparera Water Levels

Lake Waiparera is perched above the regional aquifer, thus it is hydrologically disconnected to the groundwater system. No change is expected in the hydrological functionality of the lake due to deep groundwater pumping.

Assessment of Effects

The factual data presented in this report will be considered in the context of an assessment of effects under the Resource Management Act in a companion document.

7. References

- Edwards, M., 1996, Elimination of adaptive grid interface errors in the discrete cell centred pressure equation: *Journal of Computational Physics*, v. 126, article no. 0143, p. 356–372.
- D.L. Hicks, D.J. Campbell, and I.A.E. Atkinson, 2001. Options for managing the Kaimaumau wetland, Northland, New Zealand. *SCIENCE FOR CONSERVATION* 155.
- Isaac, M.J. (compiler), 1996: Geology of the Kaitaia area. Institute of Geological & Nuclear Sciences 1:250 000 geological map 1. 1 sheet + 43 p. Lower Hutt, New Zealand. GNS Science.
- Kruseman, G. P., & de Ridder, N. A. (1979). Analysis and evaluation of pumping test data (No. TD403. K38 1983.). The Netherlands: International Institute for Land Reclamation and Improvement.
- Lincoln Agritech, 2015. Aupouri Aquifer Review. Consultancy report prepared for Northland Regional Council.
- Panday, Sorab, Langevin, C.D., Niswonger, R.G., Ibaraki, Motomu, and Hughes, J.D., 2013, MODFLOW–USG version 1: An unstructured grid version of MODFLOW for simulating groundwater flow and tightly coupled processes using a control volume finite-difference formulation: U.S. Geological Survey Techniques and Methods, book 6, chap. A45, 66 p
- SKM, 2007a. Awanui Artesian Aquifer Numerical Modelling. Consultancy report prepared for Northland Regional Council.
- SKM, 2007b. King Avocado Orchard Groundwater Take Consent Application (AEE Final). Consultancy report prepared for King Avocado Limited.
- SKM, 2010. Sweetwater Station Water Take Hearing - Response to Section 92 request. Consultancy report prepared for Landcorp Farming Limited and Te Runanga O Te Rarawa.
- Stringfield, V. T. (1966). Artesian water in Tertiary limestone in the southeastern states (No. 517-519). US Government Printing Office.
- Van Genuchten, M. Th. 1980. A closed-form equation for predicting the hydraulic conductivity of unsaturated soils. *Soil. Sci. Soc. Am. J.* 44:892—898.
- Martindale (2014). Mapping groundwater discharge into rivers using radon. Retrieved January 30, 2017, from <https://www.gns.cri.nz/Home/Our-Science/Environment-and-Materials/Groundwater/Project-Examples/Mapping-groundwater-discharge-into-rivers-using-radon>.
- Moore, R., & Wondzell, S. M. (2005). Physical hydrology and the effects of forest harvesting in the Pacific Northwest: a review. *JAWRA Journal of the American Water Resources Association*, 41(4), 763-784.
- Mulder, P. J. M. 1983. Rapportage putproef Hoogezand. Dienst Grondwaterverkenning TNO, Delft, OS.83 – 24, 7p.
- Mulder, P.J.M. 1983. Rapportage putproef Hoogezand. Dienst Grondwaterverkenning TNO Delft
- Science, GNS. Radon. Retrieved January 30, 2017, from <https://www.gns.cri.nz/Home/Services/Laboratories-Facilities/Tritium-and-Water-Dating-Laboratory/Introduction-to-Water-Dating-and-Tracer-Analysis/Radon>.
- Wildlands Consultants (2011). Ranking of top wetlands in the northland region stage 4 - rankings for 304 wetlands. Report prepared for Northland Regional Council.
- Wetlands Classification and Types. (2016, October 26). Retrieved April 06, 2017, from <https://www.epa.gov/wetlands/wetlands-classification-and-types#bogs>
- Williamson Water Advisory (2017). Motutangi-Waiharara Groundwater Model Factual Technical Report. Consultancy report prepared for Motutangi-Waiharara Water User Group.



Williamson Water Advisory (2018). Sweetwater Farms PB2 Test Pumping Report. Consultancy Report prepared for Sweetwater Farms Limited.

Appendix A. Summary of Aquifer Hydraulic Properties

The following tables summarise hydraulic property values that have been measured and estimated in models across the Aupouri Peninsula from various reports since 2000.

Table A1. Analysis of aquifer test data (Lincoln Agritech, 2015).

Pump	Screen depth	Test name	Lithology	T	B	Kx	S	K'/B'	B'	K'z
	(mBGL)			(m ² /d)	(m)	(m/d)	(-)	(d)	(m)	(m/d)
200048	18.8	Hukatere 1	Sand	60	6.4	9.4	0.0017	0.1475	13.5	2.0
200048	18.8	Hukatere 1	Sand	60	6.4	9.4	0.0107	0.2927	13.5	4.0
200048	18.8	Hukatere 3	Sand	50	6.4	7.8	0.0022	0.1909	13.5	2.6
200048	18.8	Hukatere 3	Sand	62	6.4	9.7	0.0154	0.1909	13.5	2.6
200060	64	Browne	Sand	400	10.4	38.5	0.0004	0.0014	21.2	0.03
200081	31.2	Ogle Drive	Sand	7.4	8.1	0.9	0.0467	0.8771	10.2	8.9
200229	73	Fitzwater	Shell/sand	130	6	21.7	0.0002	0.0001	26.0	0.004
200229	73	Fitzwater	Shell/sand	110	6	18.3	0.0004	0.0004	11.0	0.004
201025	27	Sweetwater	Sand	52	6.3	8.3	0.0004	0.0018	11.0	0.02
201037	27.2	Welch	Sand/shell	9	1.8	5	0.0005	0.0087	11.9	0.1
209606	110.5	King Avo	Shell	305	26	11.7	0.0007	0.0003	15.5	0.004
209606	110.5	King Avo	Shell	370	17	21.8	0.0011	0.0003	15.8	0.005
			Min	7.4	1.8	0.9	0.0002	0.0001	10	0.004
			Mean	135	8.9	13.5	0.0067	0.14	15	1.7
			Max	400	26	38.5	0.0467	0.88	26	8.9

Table A2. Analysis of aquifer test data (HydroGeo Solutions, 2000).

NRC Bore	Depth	Top of screen	Aquifer type	SWL	T	K	S
	(m)	(mBGL)		(mBGL)	(m ² /d)	(m/s)	(-)
43	55	52	Fine sand	9.3	240 - 280	6E-05 to 7.1E-05	-
48	67	19	Med sand	5.3	80 - 300	6.1E-05 to 7.1E-05	0.01-0.001
59 (s)	6	-	Fine sand	2.8	140	5.10E-04	-
59 (d)	55	49	Fine sand	13.4	190	5.30E-05	-
60	60	-	Fine sand	14.9	220 - 850	5.6E-06 to 1.3E-04	-
81	32	31	Fine sand	20.9	12 - 28	1.25E-05 to 2.9E-05	0.07-0.03
152	66	60	Fine sand	30.1	260	8.40E-05	-
184	110	101	Shelly sand	17.2	140 - 340	1.7E-05 to 4.2E-05	-
229 (211)	79	70	Shelly sand	2.6	140	2.10E-05	1.4E-04 to 1.8E-03
230	88	63	Shelly sand	4.6	240 - 310	4.3E-05 to 3.3E-05	-

NRC Bore	Depth	Top of screen	Aquifer type	SWL	T	K	S
	(m)	(mBGL)		(mBGL)	(m ² /d)	(m/s)	(-)
1007	50	45	Fine sand	33.7	275 -305	2.1E-04 to 1.9E-04	-
1025	30	27	Fine sand	1.55	60 -103	2.2E-05 to 3.7E-05	2.5E-04 to 5.0E-04
1374	32	26.6	Fine sand	0.8	48	1.80E-05	1.0E-05 to 2.0E-05
1424*	82	70	-	-	260	-	-

Table A3. Summary of aquifer test data (SKM, 2010).

Bore Owner	Well ARC No	Easting (NZMG)	Northing (NZMG)	Test Type	Test Dur. (hrs)	Rate (m ³ /day)	Obs. Bores	Screen Geology	K (m/s)	Information Source
King	201374	2533400	6681500	Constant Rate	24	576	Yes (1)	Shell	1.8E-05	HydroGeo Solutions (2000)
Sweetwater Orchards	201424	2529558	6684434	Constant Rate	72	1,176	Yes (1)	Shell	1.9E-04	Woodward Clyde (1998)
Kaurex Corporation	200230	2530331	6697328	Constant Rate	9.5	273	No (PB only)	Shell	4.3 – 3.3E-05	HydroGeo Solutions (2000)
Matai Orchards	201507	2529399	6691299	Constant Rate	88.5	497	Yes (1)	Shell	4.0 – 2.0E-04	SKM (2007)
Hopkins	200184	2520300	6706800	Constant Rate	24	260	No (PB only)	Shell	4.2 – 1.7E-05	HydroGeo Solutions (2000)
Fitzwater	200229	2529743	6690648	Constant Rate	24	864	Yes (4)	Shell	2.1 – 1.4E-04	HydroGeo Solutions (2000) and SKM (2007)
Brown	200060	2521699	6706300	Constant Rate	22	708	Yes (3)	Sand	5.6E-06 – 1.3E-04	HydroGeo Solutions (2000)
Hogg	201007	2528300	6685799	Constant Rate	20.9	160	No (PB only)	Sand	2.1 – 1.9E-04	HydroGeo Solutions (2000)
Waiharara	209499	2528580	6690100	Constant Rate	91	1,113	Yes (2)	Shell	2.0E-04	SKM (2007)
King Avocado Ltd	209606	2527482	6690562	Constant Rate	168	2,393	Yes (3)	Shell	4.3 – 1.5E-04	SKM (2007)
Hamilton Nurseries	201025	2531401	6684155	Constant Rate	6	300	Yes (2)	Sand	1.2E-04	SKM (2001)
Stanisich Orchard	200192	2528600	6695799	Constant Rate	1	1,442	No (PB only)	Shell	5.0E-05	SKM (2002a)
Terra Nova Orchard	200335	2521199	6706499	Constant Rate	39	674	Yes (6)	Shell	4.0 – 3.0E-04	SKM (2002b)
Northland Catchment Commission	200048	2519855	6701857	N/A	N/A	N/A	N/A	Sand	7.1 – 6.1E-05	HydroGeo Solutions (2000)
Northland Catchment Commission	200081	2528583	6689795	N/A	N/A	N/A	N/A	Sand	2.9 – 1.25E-05	HydroGeo Solutions (2000)

Colville	200059	2521792	6705887	Step (4)	22.3	63 - 233	No (PB only)	Sand	5.3E-05	HydroGeo Solutions (2000)
Fraser	201002	2525552	6671053	Step (3)	22	89 - 163	No (PB only)	Sand	3.0E-04	NRC database
Richards Enterprises	200043	2522513	6708792	Step (4)	19	149 - 333	No (PB only)	Sand	7.1 – 6.0E-05	HydroGeo Solutions (2000)
Herbert	200152	2528178	6688977	Step (4)	20	127 - 319	No (PB only)	Sand	8.4E-05	HydroGeo Solutions (2000)

Table A4. Calibrated model parameters (SKM, 2007a).

Material ID	Hydraulic Conductivity		Vertical anisotropy	Sy
	(m/d)	(m/s)		
Loose dune sand	10	1.20E-04	10	0.2
Weathered dune sand	6	6.90E-05	10	0.2
Fine sand	3	3.50E-05	25	0.25
Peat and sand	0.1	1.20E-06	30	0.2
Upper alluvium	0.55	6.40E-06	10	0.3
Alluvium	0.06	6.90E-07	20	0.05
Shell bed	50	5.80E-04	2	0.3

Table A5. Aquifer hydraulic parameters derived from SKM102PB test pumping (SKM, 2007b).

Bore	T	K	
	(m ² /s)	(m/d)	(m/s)
SKM101b	3.70E-03	32	3.70E-04
SKM102b	1.50E-03	13	1.50E-04
SKM103b	3.50E-03	30	3.50E-04
SKM104b	4.30E-03	37	4.30E-04

Table A6. Material parameters used within PLAXIS geotechnical subsidence model (SKM, 2007b).

King Avocado Orchard Groundwater Take Consent Application (AEE Final)							
Material	Density (KN/m ³)		Permeability (m/d)		Stiffness (kN/m ²)	Cohesion (kN/m ²)	Friction Angle (°)
	δ _{unsat}	δ _{sat}	K _x	K _y	E50ref	c _{ref}	φ
Loose Dune Sand	15	17	5	0.25	10000	0.2	28

Compact Dune Sand	17	19	0.7	0.07	15000	0.2	28
Shell Bed	18	20	22	2.2	30000	1	30

Table A7. Hydrogeological data calculated from pumping tests (WWA, 2017).

Farm	Rate (L/s)	Bore	Screen Depth (mBGL)	Method	T (m ² /d)	S (-)	B (m)	K (m/d)	K (m/s)
Stanisich Farm	25	Pumping bore	87-101	Single well Jacob	485	-	14	35	4.1E-04
				Theis Recovery	512	-		37	4.3E-04
	-	Monitoring bore	77-85	Theis (point match)	356	0.0044	8	45	5.2E-04
Honeytree Farm	29	Pumping bore	62-68, 68-71,84-93	Single well Jacob	618	-	18	34	3.9E-04
				Theis Recovery	511	-		28	3.2E-04
	-	Monitoring bore	63-69, 69-72,86-95	Theis (point match)	751	0.0003	18	42	4.9E-04
				Cooper Jacob	784	0.0003		44	5.1E-04
De Bede Farm	2.3	Pumping bore	91-97	Single well Jacob	377	-	6	63	7.3E-04
				Theis Recovery	363	-		61	7.1E-04
					Max	0.0044		63	7.3E-04
					Min	0.0003		28	3.2E-04
					Mean	0.0016		43	5.0E-04

Table A8. Calculated hydrogeological property from Single well Jacob method (WWA, 2017).

Farm	Q (L/s)	Bore	Screen Depth (mBGL)	Evaluation time (s)	T (m ² /d)	B (m)	K (m/d)	K (m/s)	Time (s) evaluation criteria	
									Minimum	Maximum
Stanisich	25	Pumping bore	87-101	210 - 1200	471	14	34	3.9E-04	183	1728
De Bede	2.3	Pumping bore	91-97	330 - 1470	273	6	46	5.3E-04	86	1728

Table A9. Estimated hydrogeological parameters from Hantush – Jacob method (WWA, 2017).

Bore	T	K _h	K _h	K'/B'	S _s
	m ² /d	m/d	m/s	d ⁻¹	m ⁻¹
Stanisich observation bore 2 (monitoring bore)	138	10	1.14E-04	1.83E-03	1.55E-04
	408	29	3.38E-04	1.35E-03	3.07E-04
	348	25	2.88E-04	7.36E-04	3.13E-04
Honeytree farm production bore 1 (monitoring bore)	579	32	3.72E-04	1.50E-04	1.63E-05
	484	27	3.11E-04	2.84E-04	2.17E-05
	707	39	4.54E-04	5.09E-05	1.70E-05

Table A10. Calibrated Model Parameters (WWA, 2017).

Model Geological Units	Model Layer	K _x		Vertical Anisotropy (-)	S _v (-)	S _s (m ⁻¹)
		(m/d)	(m/s)			
Coastal sand	1	4.5	5.2E-05	70	0.3	-
Weathered sand	1	2.8	3.2E-05	90	0.25	-
Plain zone	1	0.1	1.2E-06	15	0.01	-
Coastal sand	2&3	4	4.6E-05	30	-	0.0005
Weathered sand	2&3	3	3.5E-05	80	-	0.0005
Shellbed	4	35	4.1E-04	1	-	0.0016
Sand	5	6	6.9E-05	30	-	0.0005
Shellbed	6	22	2.5E-04	1	-	0.0016

Table A11. Test pumping results for Sweetwater Farms (WWA, 2018).

Test	Analysis	Pumping rate		Screen length m	Transmissivity (T) m ² /d	Hydraulic conductivity (K) m/s	Specific storage (/m)
		L/s	m ³ /d				
Constant pumping	PB6 Cooper-Jacob	64	5,495	17	5,700	3.9E-03	9.6E-04
	PB2 Cooper-Jacob	64	5,495	17	430	2.9E-04	-
Recovery	PB2 Theis	64	5495	17	354	2.4E-04	-

Appendix B. Recharge Modelling

B.1 Model Parameters

The soil moisture water balance model (SMWBM) is a deterministic lumped parameter model originally developed by Pitman (1976) to simulate river flows in South Africa. The code was reworked into a Windows environment and the functionality extended to include a surface ponding function, additional evaporation functions and an irrigation module.

The model utilises daily rainfall and potential evaporation data to calculate soil moisture conditions and the various components of the catchment water balance under natural rainfall or irrigated conditions. The model operates on a time-step with a maximum length of daily during dry days, with smaller hourly time-steps implemented on wet days.

The model incorporates parameters that characterise the catchment in terms of:

- interception storage,
- evaporation losses,
- soil moisture storage capacity,
- plant available water capacity,
- soil infiltration,
- sub-soil drainage;
- vadose zone vertical drainage'
- surface runoff (quickflow);
- stream baseflows (groundwater contribution); and
- the recession and/or attenuation of groundwater and surface water flow components, respectively.

B.2 Fundamental Operation

The fundamental operation of the model is as follows and in **Table B1**:

When a rainday occurs, daily rainfall is disaggregated into the hourly time-steps based on a pre-defined synthetic rainfall distribution, which includes peak intensities during the middle of the storm. This time stepping approach ensures that rainfall intensity effects and antecedent catchment conditions are considered in a realistic manner by refined accounting of soil infiltration, ponding and evaporation losses.

Rainfall received must first fill a nominal interception storage (PI – see below) before reaching the soil zone, where the net rainfall is assessed as part of the runoff/infiltration calculation.

Water that penetrates the soil fills a nominal soil moisture storage zone (ST). This zone is subject to evapotranspiration via root uptake and direct evaporation (R) according to the daily evaporation rate and current soil moisture deficits. The soil moisture zone provides a source of water for deeper percolation to the underlying aquifer, which is governed by the parameters FT and POW.

If disaggregated hourly rainfall is of greater intensity than the calculated hourly infiltration rate (ZMAX, ZMIN) surface runoff occurs. Surface runoff is also governed by two other factors, which are the prevailing soil moisture deficit and the proportion of impervious portions of the catchment directly linked to drainage pathways (AI).

Rainfall of sufficient intensity and duration to fill the soil moisture storage results in excess rainfall that is allocated to either surface runoff or groundwater percolation depending on the drainage and slope characteristics of the catchment (DIV).

Finally, the model produces daily summaries of the various components of the catchment water balance and calculates the combined surface runoff/percolation to groundwater to form a total catchment discharge.

Table B1. Summary of SMWBM parameters and value assignments for this study.

Parameter	Name	Parameter Values			Description
		Coastal sand	Weather-ed sand	Plain zone	
ST (mm)	Maximum soil water content.	178.5	178.5	100	ST defines the size of the soil moisture store in terms of a depth of water. ST is approximately equivalent to root zone depth divided by soil porosity.
SL (mm)	Soil moisture content where drainage ceases.	0	0	0	Soil moisture storage capacity below which sub-soil drainage ceases due to soil moisture retention.
ZMAX (mm/hr)	Maximum infiltration rate.	20	20	5	ZMAX and ZMIN are nominal maximum and minimum infiltration rates in mm/hr used by the model to calculate the actual infiltration rate ZACT. ZMAX and ZMIN regulate the volume of water entering soil moisture storage and the resulting surface runoff. ZMIN is usually assigned zero. ZMAX is usually assigned the saturated infiltration rate from field testing. ZACT may be greater than ZMAX at the start of a rainfall event. ZACT is usually nearest to ZMAX when soil moisture is nearing maximum capacity.
ZMIN (mm/hr)	Minimum infiltration rate.	0	0	0	
FT (mm/day)	Sub-soil drainage rate from soil moisture storage at full capacity.	5	3.8	0.8	Together with POW, FT (mm/day) controls the rate of percolation to the underlying aquifer system from the soil moisture storage zone. FT is the maximum rate of percolation through the soil zone.
POW (>0)	Power of the soil moisture-percolation equation.	2	2	2	POW determines the rate at which sub-soil drainage diminishes as the soil moisture content is decreased. POW therefore has significant effect on the seasonal distribution and reliability of drainage and hence baseflow, as well as the total yield from a catchment.
AI (-)	Impervious portion of catchment.	0	0	0.01	AI represents the proportion of impervious zones of the catchment directly linked to drainage pathways.
R (0,1,10)	Evaporation-soil moisture relationship	0	0	0	Together with the soil moisture storage parameters ST and SL, R governs the evaporative process within the model. Three different relationships are available. The rate of evapotranspiration is estimated using either a linear (0,1) or power-curve (10) relationship relating evaporation to the soil moisture status of the soil. As the soil moisture capacity approaches full, evaporation occurs at a near maximum rate based on the mean monthly pan evaporation rate, and as the soil moisture capacity decreases, evaporation decreases according to the predefined function.
DIV (-)	Fraction of excess rainfall allocated directly to pond storage.	0	0	0	DIV has values between 0 and 1 and defines the proportion of excess rainfall ponded at the surface due to saturation of the soil zone or rainfall exceeding the soils infiltration capacity to eventually infiltrate the soil, with the remainder (and typically majority) as direct runoff.
Kv (m/s)	Vertical hydraulic conductivity	8E-6	5E-6	2E-8	Kv along with the VGn parameter and the soil moisture status governs the unsaturated hydraulic conductivity and travel times within the vadose zone.

VGn (-)	van Genuchten parameter	2.68	2.68	1.09	Defines the soil moisture to unsaturated conductivity relationship according to van Genuchten's equation.
VPor (-)	Average porosity of the vadose zone	0.15	0.15	0.40	This is typically fixed and not changed during calibration as changes can easily be compensated for in Kv.
D (m)	Average depth of the vadose zone	10	10	1	The deeper the vadose zone, the longer the travel times.
TL (days)	Routing coefficient for surface runoff.	1	1	1	TL defines the lag of surface water runoff. This is not necessary to define for this study as we are only interested in the groundwater percolation component of the water balance.
GL	Groundwater recession parameter.	1	1	1	GL governs the lag in groundwater discharge or baseflow from a catchment.

B.3 Vadose zone discharge functionality

Based on the simulated groundwater percolation from the soil moisture model, the vadose zone discharge functionality was utilised to simulate the vertical movement of water in the unsaturated zone. The depth and hydraulic properties of the vadose zone govern the delay in groundwater response to climate variation.

The vadose zone functionality built into the SMWBM is premised on three principals:

1. **Unsaturated hydraulic conductivity** - The van Genuchten (1980) equation was used to determine unsaturated hydraulic conductivity in the vadose zone, which is governed by the saturated hydraulic conductivity that sets the upper value, and the degree of saturation in the soil zone as a proxy for general sub-surface degree of wetness.
2. **Vertical flux rate** - The simplified Richard's equation is used to estimate the vertical flux rate of water, which is assumed to be driven by gravitational force (only) and therefore governed by unsaturated hydraulic conductivity and porosity.
3. **Transport time** - The Muskingum equation was used to translate the vertical flux into a routing scheme, using the depth of the vadose zone and vertical flux rate (velocity) as the time component of the equation.

The delay in groundwater recharge was observed for coast sand, weathered sand and peat and clay to different extents. The simulated results for weathered sand suggest that the groundwater recharge has approximately 2-3 months delay in responding to the rainfall variation, depending on locality. **Figure B1.** provides an example of the functionality of the vadose zone model.

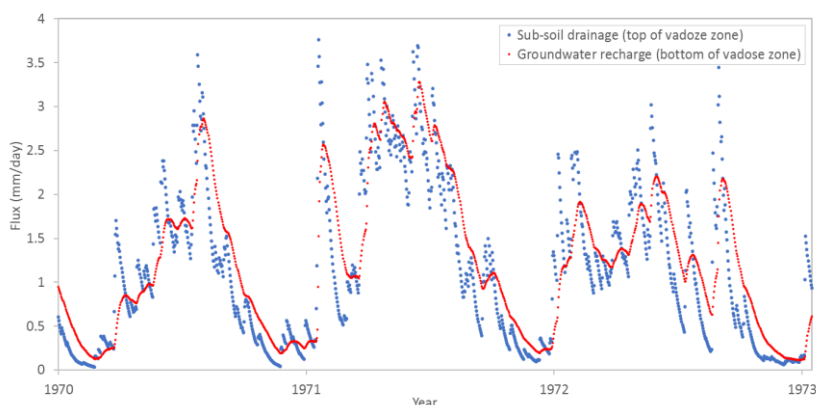


Figure B1. Graph comparing inputs and outputs from vadose zone model.

Appendix C. Irrigation Scheduling and Actual Irrigation Use

C.1 Development of an irrigation scheduling dataset

The irrigation module of Soil Moisture Water Balance Model was utilised to optimise irrigation applications for avocado orchards in the area and to provide input into the transient irrigation scenario for groundwater modelling purposes. The parameters and associated values used in the model are shown in **Table C1**.

Table C1. Summary of parameters used in the irrigation model

Parameter	Description	Values	Basis of Values
Maximum Soil Moisture Content (ST)	The capacity of water in mm in the soil at field capacity.	178.5	Estimated from potential rooting depth (PRD) and macroporosity (n). $ST = PRD \times n/100$. 1190 mm x 15%= 178.5 mm
Plant Available Water (PAW)	The amount of water physically accessible by the plants in the root zone in mm.	125	Table 22 of Crop Evapotranspiration - Guidelines for Computing Crop Water Requirements from the Food and Agricultural Organisation of the United Nations (FAO) ¹ states that 70% of Total Available Soil Water (interpreted as equivalent to ST in the SMWBM) can be depleted before the point where avocado trees suffer stress. Therefore, $PAW = 0.7 \times ST$
Allowable Deficit (AD)	Soil moisture level where irrigation ceases.	90% of PAW	The avocado is very flood-sensitive with even short periods of waterlogging resulting in reduced shoot growth, altered mineral uptake and root death. To avoid flooding and surface runoff, soil moisture levels during irrigation should not exceed 90% of field capacity.
Minimum/ Critical Deficit (CD)	Percentage of PAW at which further drying of soil would start to have an impact on plant growth rates, and hence CD represents the soil moisture level at which irrigation commences.	40% of PAW	The rule of thumb for critical deficit is 50% of PAW. However, a grower aiming to maximise crop yield may want a small critical deficit of only 20% (80% PAW) ² . A balance is also required between a small critical deficit (high soil moisture levels) and water wastage, which results under high moisture conditions when rainfall occurs during summer. Through trial and error, we have used CD values of 40% PAW.
Peak Application Depth	Maximum daily irrigation depth applied to soil (mm/day).	4.0 mm	Selected through optimisation target of minimisation in losses, while maintaining moisture levels at or above the CD. Note. This is the amount of irrigation water reaching the soil surface, which is less than the amount applied by the irrigator <i>per se</i> . due to application inefficiencies (losses).
Application Duration	Duration in hours over which the peak application depth is applied	2 hours	Data estimated
Rain Threshold	Daily rainfall total in mm when a farmer would choose not to irrigate.	10 mm	Judgement
Season	Irrigation season start and finish	October – April	General irrigation season length.

The same historical rainfall record from 01/08/1956 to 31/08/2016 described in **Appendix B** was used in the model. The simulated soil moisture content with/without irrigation are shown in **Figure C1**.

¹ <http://www.fao.org/docrep/x0490e/x0490e0e.htm>

² Anon. Scheduling overview. NZ Avocado Industry 11 Mar 2010. (accessed 16 Jul 2015) <<http://www.hortinfo.co.nz/factsheets/fs110-68.asp>>.

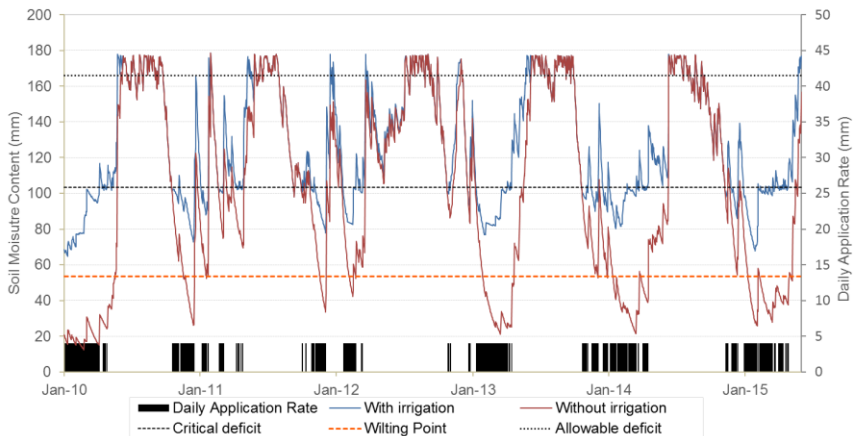


Figure C1. Irrigation simulation output for time period 2010-2015

The daily peak application rate was optimised through a set of simulations, aiming to minimize the water losses through surface runoff and percolation to groundwater system, while maintaining a soil moisture content that is above the plant critical deficit.

The simulations indicate an optimized peak application rate of 4 mm/day. The relationship between annual irrigation amount and peak application rate is shown in **Figure C2**.

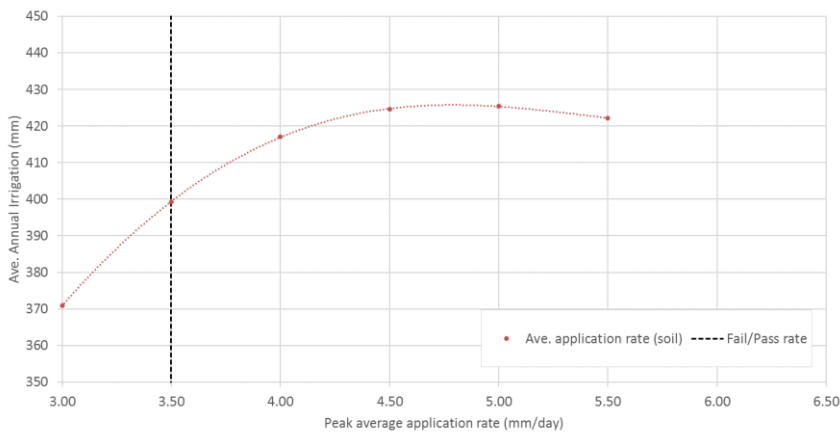


Figure C2. Assessment of peak application rate that is water conservative for sandy soils.

The irrigation demand was simulated for the period of 01/08/1956 to 31/08/2016 and a summary graph showing the number of days irrigation was required per season is shown in **Figure C3**.

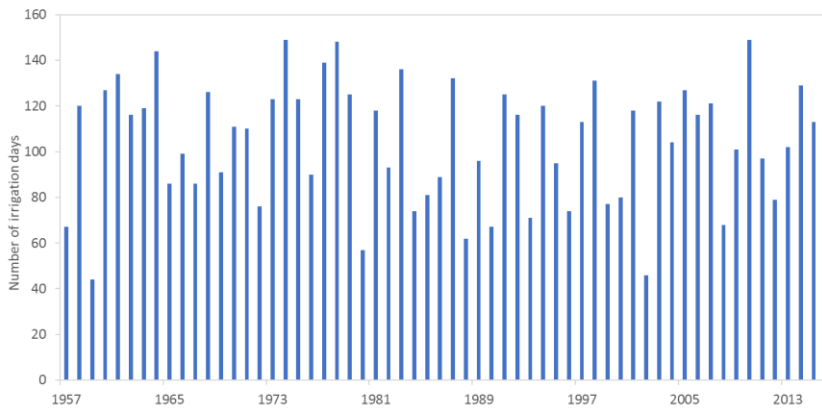


Figure C3. Simulated number of irrigation days per season.

The statistical distribution of monthly irrigation application totals, with 10% additional water added to account for irrigation inefficiency, is shown in **Figure C4**.

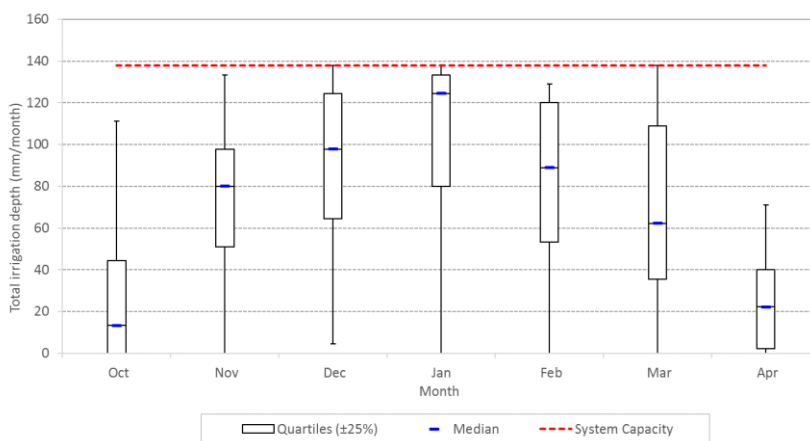


Figure C4. Seasonal irrigation demand for sandy soil.

The annual irrigation demand volume and commensurate number of days of irrigation was calculated and it was found that the 90%ile of simulated annual demand is equivalent to approximately 150 days pumping at the peak rate. This closely aligns with the annual volumes specified in consents granted.

C.2 Development of an irrigation actual use dataset

The simulated irrigation demand time series was applied to one of the currently consented groundwater bores with a peak allocation rate of 720 m³/day owned by Ivan Stanisich (NRC consent No. CON20102739101). The total amount of demand simulated during the irrigation period was calculated and compared with available historical use records, as shown in **Figure C5**.

The simulated demand varies with climate conditions from a minimum of 44 days irrigation to a maximum of 149 days irrigation during the irrigation season. For the years where records were available for comparison, measured demand is approximately 30% of simulated demand. There are a number of minor reasons for this including human operational decision and actual rainfall not being totally consistent with site rainfall, but the primarily reason is that the orchard is not fully developed.

Considering the scope and purpose of this modelling, this irrigation demand time series is a conservative estimate and therefore appropriate to use in effects assessment from the abstraction of groundwater.

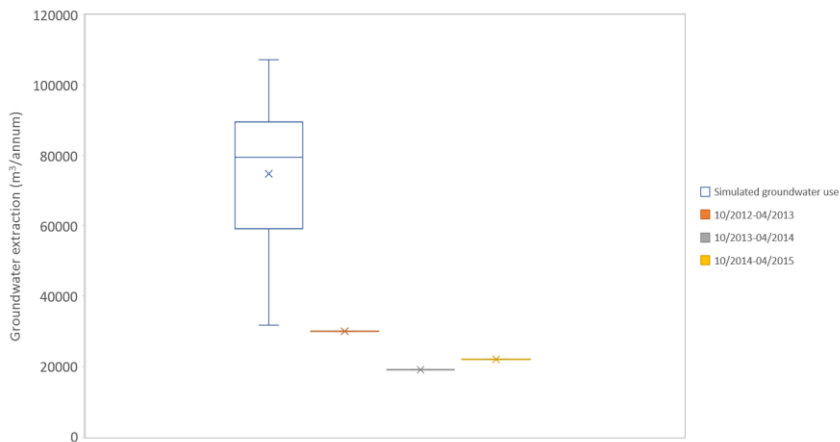
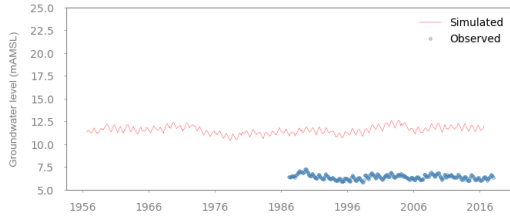


Figure C5. Comparison between the simulated groundwater demand and the historical records.

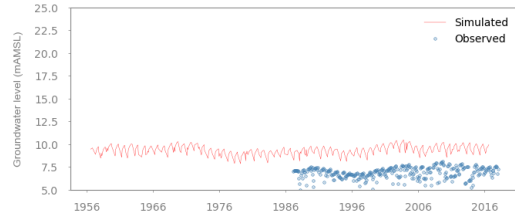
The irrigation demand pattern from **Section C.1** was applied to all the groundwater irrigation bores in the model area to construct transient pumping time series input for the model.

Appendix D. Calibrated Model Hydrographs

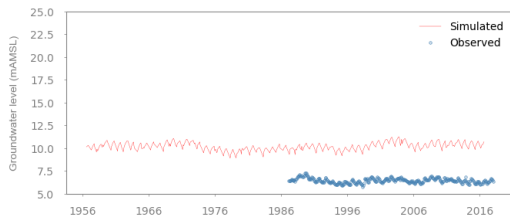
Paparore (18 m)



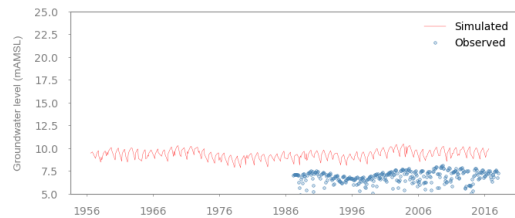
Paparore (65 m)



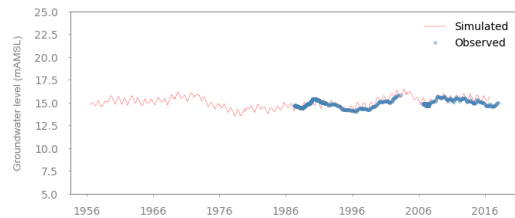
Paparore (35 m)



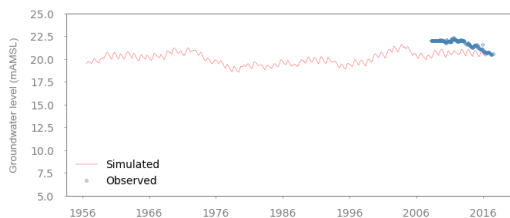
Paparore (75 m)



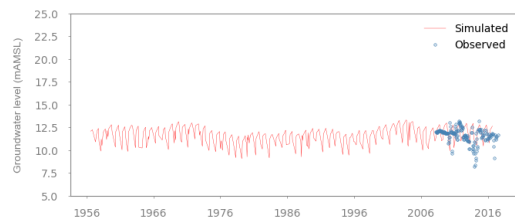
Ogle Drive



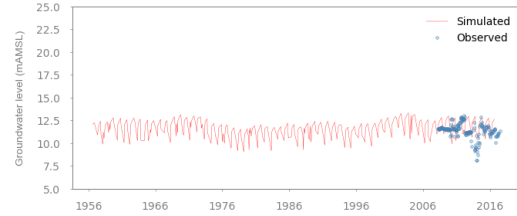
Valic-1 (Shallow Monitoring)



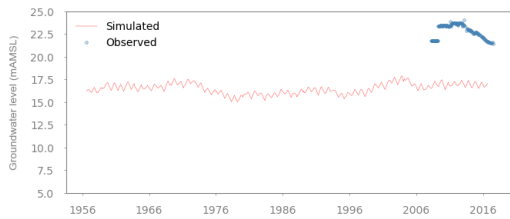
Valic-1 (Deep Monitoring)



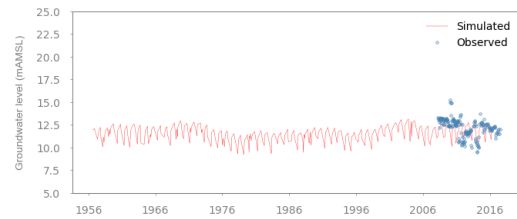
Valic-1 (Deep Production)



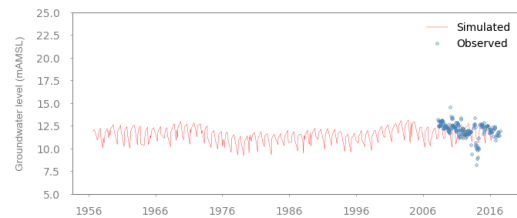
Valic-2 (Shallow Monitoring)



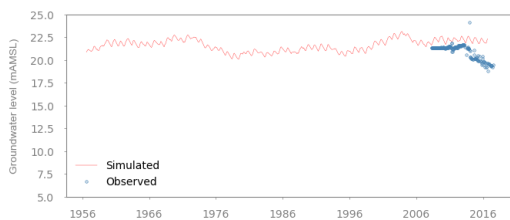
Valic-2 (Deep Monitoring)



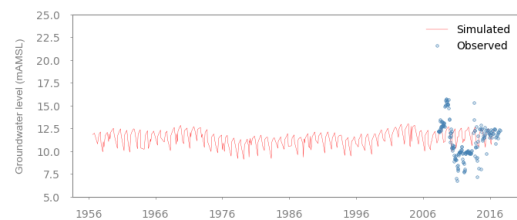
Valic-2 (Deep Production)



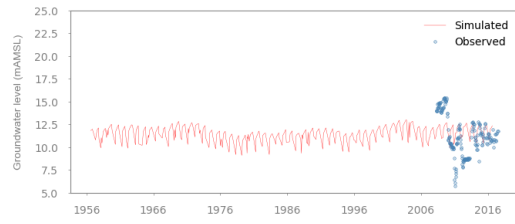
Valic-3 (Shallow Monitoring)



Valic-3 (Deep Monitoring)

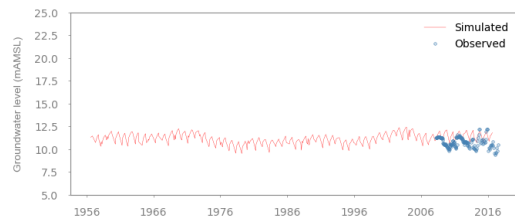
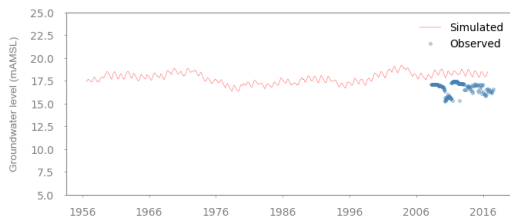


Valic-3 (Deep Production)



Valic-4 (Deep Monitoring)

Valic-4 (Shallow Monitoring)



Valic-4 (Deep Production)

Figure D1. Hydrographs of simulated versus observed groundwater levels.